Fermi National Accelerator Laboratory

FERMILAB-Pub-91/323-A
November 1991
(submitted to *Physical Review D*)

Gravitational Radiation from Colliding Vacuum Bubbles

Arthur Kosowsky, Michael S. Turner, and Richard Watkins

NASA/Fermilab Astrophysics Center
Fermi National Accelerator Laboratory
Batavia, IL 60510-0500

and

Departments of Physics and Astronomy & Astrophysics
Enrico Fermi Institute
The University of Chicago
Chicago, IL 60637-1433

Abstract. In the linearized-gravity approximation we numerically compute the amount of gravitational radiation produced by the collision of two true-vacuum bubbles in Minkowski space (these two approximations are valid for $\tau \lesssim H^{-1}$). The bubbles are separated by distance d and we calculate the amount of gravitational radiation that is produced in a time $\tau \sim d$ (in a cosmological phase transition τ corresponds to the duration of the transition, which is expected to be of the order of the bubble separation d). We find that the amount of gravitational radiation produced depends only upon the grossest features of the collision: the time τ and the energy density associated with the false-vacuum state, $\rho_{\rm vac}$. In particular, the spectrum $dE_{\rm GW}/d\omega \propto \rho_{\rm vac}^2 \tau^6$ and peaks at a characteristic frequency $\omega_{\rm max} \simeq 3.8/\tau$, and the fraction of the vacuum energy released into gravitational waves is about $1.3 \times 10^{-3}(\tau/H^{-1})^2$, where $H^2 = 8\pi G\rho_{\rm vac}/3$ (τ/H^{-1} is expected to be of the order of a few per cent). We address in some detail the important symmetry issues in the problem, and how the familiar "quadrupole approximation" breaks down in a most unusual way: It *overestimates* the amount of gravitational radiation produced in this highly relativistic situation by more than a factor of 50. Most of our results are for collisions of bubbles of equal size, though we briefly consider the collision of vacuum bubbles of unequal size. Our work implies that the vacuum-bubble collisions associated with a strongly first-order phase transitions are a very potent cosmological source of gravitational radiation.

Operated by Universities Research Association Inc. under contract with the United States Department of Energy

I. Introduction

Gravitational radiation from cosmological processes may be a rich source of information about the early Universe. Though efforts to detect gravity waves directly have not yet born fruit, the "menu" of sources—many of which cannot be probed by other means—have made clear the impact that gravitational wave astronomy might have on both cosmology and astrophysics [1]. Pulsar timing data and the smoothness of the cosmic microwave background already place limits on the amplitude of the radiation, and a new generation of detectors—laser interferometric devices (LIGOs) and improved resonance bar detectors—are planned for the near future [1,2].

Point sources of gravitational radiation will be of most interest to astrophysicists; however, for cosmology the stochastic background of gravity waves which exists today will be of the greatest interest. Just as the blackbody microwave background is a remnant of the early history of our Universe ($z \sim 1000$, $t \sim 300,000$ yr), the gravity-wave background is as well. However, its character is radically different from the microwave background. Thermal decoupling of gravitons presumably occurred at the Planck epoch ($T \sim 10^{19}$ GeV, $t \sim 10^{-43}$ sec), much earlier than decoupling of photons, so the resulting black-body spectrum is at a lower temperature than the microwave background ($\lesssim 1$ K). If the Universe went through an inflationary phase, the black-body graviton spectrum will "red shift away" to an undetectably low temperature $T \ll 1$ K; a new spectrum arises due to quantum fluctuations [3]. More importantly, gravitational radiation produced by cosmological processes occurring after inflation is just superposed onto the stochastic background and not thermalized. Thus gravitons may provide us with a unique probe of processes occurring at very early times. Since the frequency of gravity waves produced at a given epoch is likely to be related to the Hubble time H^{-1}, the stochastic background could have the thermal history of the Universe spread across its spectrum.

Potentially important cosmological sources include cosmic strings [4], textures [5], domain-wall collisions, soliton stars [6], and phase transitions [7]. In particular, oscillating string loops produce large amounts of gravitational radiation, and timing measurements of the millisecond pulsar have been used to place stringent limits on the existence of cosmic strings [8]. While the radiation from textures has yet to be computed, their unwinding involves considerable energy densities, making them a possible strong source. First-order phase transitions can be violent, producing large energy gradients and high velocities, the necessary ingredients for a strong source of gravitational radiation. Thus far, only qualitative estimates of the amount of gravitational radiation from a first-order phase transition have been made [7].

In this paper, we initiate detailed study of the gravitational radiation produced in a strongly first-order phase transition. In such a transition, the Universe starts in a metastable false-vacuum state; bubbles of true vacuum are nucleated through either quantum or thermal tunneling. As a bubble expands, the liberated vacuum energy is converted

into kinetic energy of the bubble wall. Eventually bubbles collide, completing the transition. Clearly, this situation involves the key ingredients of concentrated energy and high velocities necessary to produce significant gravitational radiation.

Our work is motivated by a recent revival of interest in theories where inflation ends with a first-order phase transition, wherein the vacuum energy that drives inflation is eventually converted into radiation by bubble collisions [9]. Dubbed "extended" or "first-order" inflation, these models circumvent the "graceful-exit" problem that plagued old inflation by means of a time dependent expansion and/or bubble-nucleation rate. Turner and Wilczek have estimated the stochastic background of gravitational radiation produced by bubble collisions in these models and found that bubble collisions are a very potent source of gravity waves and provide a unique signature of first-order inflation [10]. Here we explore the production process in more detail, using numerical simulations of bubble collisions. Our calculations are also relevant to other first-order phase transitions in the early Universe, and this application of our work is discussed elsewhere [11].

Specifically, we compute numerically the gravitational radiation resulting from the collision of two scalar-field vacuum bubbles. We do so by evolving two bubbles classically for a time τ comparable to their separation d ($d \lesssim \tau \lesssim d$). Our calculation is done in Minkowski space, ignoring the gravitational effects of the bubbles themselves and the expansion of the Universe, but to all orders in v/c (*i.e.*, in the linearized-gravity approximation; as we shall discuss, the aforementioned assumptions are valid for $\tau, d \lesssim H^{-1}$). We find the remarkable result that the spectrum of radiation and total amount of radiation only depend upon the grossest features of the bubble collision, the vacuum energy density and the time/separation τ. In particular, the characteristic frequency of the gravity waves $\omega \simeq 3.8/\tau$, $dE_{\rm GW}/d\omega \propto {\rho_{\rm vac}}^2\tau^6$, and the fraction of the vacuum energy liberated into gravity waves by the collision of two bubbles $f \simeq 1.3 \times 10^{-3}(\tau/H^{-1})^2$, where $H^2 = 8\pi G\rho_{\rm vac}/3$.

In the next Section we commence with a detailed discussion of bubble dynamics and the symmetry issues involved in the problem. Section III covers the formalism of gravitational wave generation and several technical issues. Theoretical expectations for the gravitational wave spectrum, based upon simple scaling arguments, are presented in Section IV. Our numerical calculations and results are presented in Section V. We end with a brief discussion of bubble kinematics in a phase transition as relevant to our work, and finally a few concluding remarks. Some technical discussion and formulae are relegated to two Appendices.

II. Scalar-field Bubbles and Symmetry Issues

(a) Bubble nucleation

Consider a real scalar field φ with Lagrangian density

$$\mathcal{L} = \frac{1}{2}\partial^\mu\varphi\partial_\mu\varphi - V(\varphi), \tag{1}$$

where our metric signature is $(1,-1,-1,-1)$. We are interested in the case where the potential $V(\varphi)$ possesses two inequivalent local minima: a false- and a true-vacuum state. Throughout this paper we will use a φ^4 potential with two degenerate minima, $V_0(\varphi)$, with an additional linear term that breaks the degeneracy:

$$\begin{aligned} V_0(\varphi) &= \frac{\lambda}{8}(\varphi^2 - {\varphi_0}^2)^2, \\ V(\varphi) &= V_0(\varphi) + \epsilon\lambda{\varphi_0}^3(\varphi + \varphi_0), \end{aligned} \tag{2}$$

where ϵ measures the degree of symmetry breaking between the two minima at $\pm\varphi_0$. Figure 1 shows this potential for various values of ϵ. The relative minimum at $\varphi_+ = \varphi_0 + \mathcal{O}(\epsilon\varphi_0)$ is the "false vacuum," while the global minimum at $\varphi_- = -\varphi_0 + \mathcal{O}(\epsilon\varphi_0)$ is the "true vacuum." The difference in energy density between the false and true vacua $\rho_{\rm vac} \simeq 2\epsilon\lambda\varphi_0^4$. Classically, the false-vacuum state $\varphi = \varphi_+$ is stable, but quantum mechanical tunnelling will cause it to decay to the true-vacuum state $\varphi = \varphi_-$. This decay proceeds via quantum nucleation of true-vacuum bubbles that spontaneously appear from the false-vacuum state. Coleman has shown that the bubble with minimum action is $O(4)$-invariant [12]; the minimum-action "bounce" solution satisfies the equations

$$\varphi = \varphi(\rho), \qquad \rho = \sqrt{t_E^2 + \mathbf{x}^2}, \tag{3}$$

$$\frac{d^2\varphi}{d\rho^2} + \frac{3}{\rho}\frac{d\varphi}{d\rho} = \frac{\partial V}{\partial\varphi}, \tag{4}$$

with the boundary conditions

$$\lim_{\rho\to\infty}\varphi(\rho) = \varphi_+, \qquad \left.\frac{d\varphi}{d\rho}\right|_0 = 0, \tag{5}$$

where $t_E \equiv it$ is Euclidean time. The Euclidean action for the $O(4)$ bubble is

$$S_E = 2\pi^2\int_0^\infty \left[\frac{1}{2}\left(\frac{d\varphi}{d\rho}\right)^2 + V\right]\rho^3\,d\rho. \tag{6}$$

The most likely initial bubble configuration after the quantum nucleation event is obtained by analytically continuing the bounce solution to Minkowski space and then taking the $t = 0$ time slice. Bubbles of different sizes or profiles than the bounce solution have larger actions associated with their nucleation, and their nucleation rates are suppressed exponentially by the difference between their action and the bounce action. In any case, our results are very insensitive to the initial bubble configuration.

For orientation we quickly summarize bubble nucleation in the "thin-wall" limit, valid when the false-vacuum energy is small compared to the height of the barrier between the false and true vacua (*i.e.*, $\epsilon \ll 1$). In this approximation, it is straightforward to compute

expressions for the radius of the bubble at nucleation, R_0, and the Euclidean action for bubble nucleation, S_E [12]:

$$R_0 = \frac{3}{\rho_{\rm vac}} \int_{-\varphi_0}^{\varphi_0} d\varphi \sqrt{2V_0(\varphi)}; \tag{7a}$$

$$S_E = \frac{27\pi^2}{2{\rho_{\rm vac}}^3} \left[\int_{-\varphi_0}^{\varphi_0} d\varphi \sqrt{2V_0(\varphi)} \right]^4 ; \tag{7b}$$

$$H^2 \equiv \frac{8\pi}{3} \frac{\rho_{\rm vac}}{{m_{\rm Pl}}^2} = \frac{16\pi}{3} \frac{\epsilon\lambda\varphi_0^4}{{m_{\rm Pl}}^2}; \tag{7c}$$

Direct evaluation of the required integral gives

$$R_0 = \frac{1}{\sqrt{\lambda}\epsilon\varphi_0}; \qquad S_E = \frac{\pi^2}{3\lambda\epsilon^3}; \qquad \frac{R_0}{H^{-1}} = 4\sqrt{\frac{\pi}{3\epsilon}} \frac{\varphi_0}{m_{\rm Pl}}. \tag{8}$$

Since we expect φ_0 to be of order the GUT scale for models of extended inflation—10^{15} GeV or so—and even smaller for other phase transitions, the size of the bubble when it is nucleated should be much smaller than the horizon. This justifies the neglect of gravitational effects on bubble nucleation [13]—and as we shall see later—the neglect of the gravitational field of the bubble itself.

Once a bubble is nucleated, its evolution is determined by the usual Klein-Gordon equation for a real scalar field,

$$\frac{\partial^2\varphi}{\partial t^2} - \nabla^2\varphi = -\frac{\partial V}{\partial \varphi}. \tag{9}$$

The bubble initially has no kinetic energy. Since the interior true-vacuum region of the bubble has a lower energy than the surrounding false vacuum, an effective outward pressure exists on the walls of the bubble. This "vacuum pressure" forces the bubble to expand; the region of true vacuum becomes larger and larger. The velocity of the bubble walls asymptotically approaches the speed of light; the bubble wall becomes thinner as the surface energy density of the bubble increases. If we consider a pair of bubbles, each expands quiescently until the two bubbles collide. Since the bubble walls have large energy densities, the collision is violent. The colliding walls do not annihilate or pass through each other, but create a region where the scalar field oscillates rapidly. The collision of two vacuum bubbles is illustrated in Fig. 2.

(b) Symmetry considerations

The classical evolution of a true-vacuum bubble after its quantum mechanical nucleation possesses a high degree of symmetry. Most of the following symmetry considerations are well known [14]; here we review them in some detail because of their bearing on the present problem. The time evolution of a critical bubble is given by analytic continuation

of the $O(4)$ symmetric solution to Minkowski space and taking the $t > 0$ part. The complete solution ($-\infty < t < \infty$) corresponds to a bubble that collapsed from infinite size to a minimum size R_0 and then again expanded to infinite size. Because of the $O(4)$ symmetry of the bounce, the complete solution is $O(3,1)$ symmetric: observers in all Lorentz frames see the same thing. The symmetry implies that the field is a function only of $\mathbf{x}^2 - t^2$; if we let $\mathbf{x}_{\rm wall}$ denote a fiducial point within the bubble wall, then at time t the position of the bubble wall satisfies

$$\mathbf{x}_{\rm wall}^2 - t^2 = R_0^2, \tag{10a}$$

where R_0 is the initial bubble radius. The bubble wall moves with constant acceleration and rapidly approaches the speed of light;

$$v_{\rm wall} = \frac{1}{\sqrt{1 + R_0^2/t^2}}, \tag{10b}$$

$$\gamma_{\rm wall} = \sqrt{1 + t^2/R_0^2}. \tag{10c}$$

Note that at late times, $t \gg R_0$, the Lorentz factor γ increases as t/R_0; since the surface area of the bubble increases as $4\pi t^2$ (for $t \gg R_0$), the energy in the bubble wall increases as t^3, which is accounted for by the release of false-vacuum energy, $E_{\rm vac} \simeq 4\pi\rho_{\rm vac}t^3/3$ ($t \gg R_0$). Likewise, it is important to note that the bubble wall becomes thinner due to Lorentz contraction: $\Delta R \propto \gamma^{-1} \propto t^{-1}$, where ΔR is the wall thickness. This fact must be taken into account when selecting the grid size for numerical evolution of the scalar field.

The $t > 0$ history of the bubble is not $O(3,1)$ invariant: It corresponds to a bubble nucleated on the $t = 0$ space-like hypersurface of a specific Lorentz frame. However, in the limit that $R_0 \to 0$, the $t > 0$ history of the bubble solution *is* $O(3,1)$ invariant: It is the finite size of the bubble at $t = 0$ that defines a particular space-like hypersurface and breaks Lorentz invariance. Of course, a single vacuum bubble, due to its spherical symmetry, produces no gravitational radiation.

Now consider two $O(3,1)$ solutions with common time origins centered on the z-axis at positions $z = \pm d/2$ (in some Lorentz frame). If we neglect the interaction of the two bubbles for the moment and consider the complete histories of the two individual bubble solutions, we see that the "double-bubble" solution is $O(2,1)$ invariant (the generators of the symmetry are Lorentz boosts along the x- and y-axes and rotations about the z-axis). If we include interactions between the bubbles, the solution is still $O(2,1)$ invariant, since the scalar field equation of motion which governs the interactions is fully Lorentz invariant. However, the $t > 0$ evolution of the double-bubble solution is *not* $O(2,1)$ invariant; $O(2,1)$ invariance is broken by the finite size of the bubbles at nucleation. As in the single-bubble case, in the limit that the nucleated bubbles are of zero size ($R_0 \to 0$), the $t > 0$ history of the two bubbles is $O(2,1)$ invariant. As we shall see shortly, $O(2,1)$ invariance or noninvariance is a crucial issue.

The noninvariant Lorentz boost (along the z-axis) has the effect of changing the relative nucleation times of the two bubbles. If the $O(2,1)$ symmetry is unbroken, the general two-bubble collision is gained from the equal-bubble collision (*i.e.*, simultaneous nucleation) simply by a Lorentz boost in the z-direction. More explicitly, for two bubbles with nucleation events (t_1, z_1) and (t_2, z_2) with space-like separation, a Lorentz boost in the z-direction with velocity $\beta = (t_2 - t_1)/(z_2 - z_1)$ transforms the collision to a frame in which the bubbles are nucleated simultaneously and the problem possesses $O(2,1)$ symmetry. Conversely, for two bubbles nucleated simultaneously at $z = \pm d/2$, a Lorentz boost with velocity β results in bubbles nucleated in the boosted frame at $t = \mp\gamma\beta d/2$, $z = \pm\gamma d/2$; when the bubbles collide in the boosted frame, the ratio of their diameters will be $(1+\beta)/(1-\beta)$. In the boosted frame, we still have $O(2)$ symmetry (rotations around the z-axis); however, the additional boost symmetries in the x and y directions are now gone, since these boosts will alter the relative nucleation times of the two bubbles.

What is the significance of the $O(2,1)$ invariance? Chao [15] has shown that an $O(2,1)$ invariant space-time cannot support gravitational waves. Specifically, he demonstrates that the $O(2,1)$ invariant space-time associated with the nucleation of two bubbles of zero size is isomorphic to an $O(3)$ (Schwarzschild-de Sitter) space-time with a time-varying, spherically-symmetric stress-energy distribution. As is well appreciated, an $O(3)$ space-time does not have sufficient degrees of freedom to support gravitational radiation; to produce gravitational radiation a source must have a time-varying quadrupole (or higher) multipole moment. A more heuristic explanation of why the fully $O(2,1)$-symmetric collision of two vacuum bubbles does not produce gravitational radiation proves helpful. Clearly the collision of two vacuum bubbles is highly nonspherical; thus the absence of gravitational radiation must trace to a precise cancellation of the radiation emitted at different times and places during the collision, just as the absence of gravitational radiation in a problem with spherical symmetry traces to the cancellation of the gravitational radiation emitted by the different parts of the spherically-symmetric matter distribution. In our case the $O(2,1)$ invariance guarantees the exact cancellation; in the spherically-symmetric analogue it is the $O(3)$ invariance that guarantees it.

In order that the collision of two bubbles of true vacuum produce gravitational radiation, $O(2,1)$ invariance must be broken. In the present circumstance, the nucleation event (as mentioned above) and the end of the phase transition break the invariance. Since bubbles are expected to be far apart at the time of their nucleation (*i.e.*, $R_0 \ll d$), they are nearly spherically symmetric when nucleated, and so the first of these symmetry-breaking effects does not result in significant gravitational radiation. (In Section VI we will show that d is expected to be much greater than R_0.) In any case the amount of radiation produced increases as d^5, so that $d \gg R_0$ is the case of greatest interest.

This brings us to the important $O(2,1)$ symmetry-breaking effect, the one which allows for abundant gravitational radiation production from vacuum-bubble collisions. Ultimately we are not interested in the collision of just two bubbles of true vacuum. In realistic

scenarios where the phase transition is eventually completed, the two colliding bubbles expand outward and at some time meet up with space that is (more or less) in the true vacuum due to the nucleation, expansion, and collision of other bubbles. (Contrast this with the case of only two bubbles, where space outside the bubbles, $|x| \gtrsim t$, remains in the false vacuum.) We shall use a phenomenological cutoff to account for this fact: We compute the gravitational radiation emitted by two colliding bubbles from time $t = 0$ to time $t = \tau$, where τ is roughly the duration of the phase transition. The time cutoff breaks $O(2,1)$ symmetry since it must be specified in a particular Lorentz frame. The amount of radiation emitted will necessarily depend upon the time cutoff. The precise form of the cutoff obviously depends upon details of the phase transition. To model the cutoff, we multiply the stress-energy sources for gravitational radiation by a smooth function $C(t)$, which we take as

$$C(t) = \begin{cases} 1, & 0 \le t \le \tau_c \\ \exp[(t-\tau_c)^2/{\tau_0}^2], & \tau_c \le t \le \tau. \end{cases} \tag{11}$$

This cutoff factor smoothly ramps the sources to zero between $t = \tau_c$ and the cutoff time $t = \tau$. We generally take $\tau_c = 0.9\tau$ so that the "completion of the phase transition" takes place in the last 10% of the total time evolution of the bubbles. We also take τ_0 small enough so that the sources are essentially zero at $t = \tau$. While the cutoff is *ad hoc*, our numerical results are not sensitive to the functional form of the cutoff, and vary in a sensible way with τ_c/τ (see Sec. V). Also note that a smooth cutoff is necessary from a numerical point of view: it serves essentially as a window function for the Fourier transforms appearing in the radiation formulas derived in the following Section. An abrupt cutoff, $C(t) = \Theta(\tau - t)$ where Θ is the Heaviside function, would introduce spurious radiation that would swamp the physical signal, especially at high frequencies.

The $O(2,1)$ symmetry of the problem has very practical value. Even though the spacetime of two equal-size colliding bubbles is not globally $O(2,1)$ symmetric, the field $\varphi(\mathbf{x}, t)$ is a function of only two variables over its domain of definition [14,16]; *i.e.*, for $0 \le t \le \tau$,

$$\varphi(\mathbf{x}, t) = \varphi(t^2 - r^2, z) \tag{12}$$

where $r^2 \equiv x^2 + y^2$. Changing to hyperbolic coordinates defined by

$$t = s\cosh\psi, \quad x = s\sinh\psi\cos\theta, \quad y = s\sinh\psi\sin\theta, \qquad (t^2 > r^2) \tag{13a}$$

$$t = s'\sinh\psi', \quad x = s'\cosh\psi'\cos\theta', \quad y = s'\cosh\psi'\sin\theta', \qquad (t^2 < r^2) \tag{13b}$$

it is clear that φ is independent of ψ (ψ') and θ (θ'); that is, $\varphi = \varphi(s, z)$ or $\varphi = \varphi(s', z)$. In these coordinates the Lagrangian density and equation of motion become respectively

$$\mathcal{L} = \frac{1}{2}\Big(\frac{\partial\varphi}{\partial s}\Big)^2 - \frac{1}{2}\Big(\frac{\partial\varphi}{\partial z}\Big)^2 - V(\varphi), \tag{14}$$

$$\frac{\partial^2\varphi}{\partial s^2} + \frac{2}{s}\frac{\partial\varphi}{\partial s} - \frac{\partial^2\varphi}{\partial z^2} = -\frac{\partial V}{\partial\varphi}. \tag{15}$$

Thus the evolution of two colliding bubbles reduces to a two-dimensional problem: one spatial variable z and one time variable s. For the problem at hand, calculations using this 1+1 dimensional wave equation are much less computationally demanding and allow far greater dynamic range.

III. Generation of Gravitational Radiation

(a) Assumptions and approximations

Because of the nonlinear nature of gravity in the context of general relativity, computing gravitational radiation is more complicated than computing electromagnetic radiation [17]. In simplistic terms, the difficulty arises because the gravitational field itself (including gravitational radiation!) can act as a source. When computing electromagnetic radiation one often expands in powers of the velocity of the source, v/c. In the computation of gravitational radiation, the analogous procedure is a double expansion in terms of the strength of the gravitational potential, ϕ/c^2, and the velocity of the source, v/c. For a gravitationally bound system, the two expansion parameters are of comparable size: $\phi \sim v^2$ (the virial relation). This relation holds for most astrophysical sources; however it certainly does not hold for the collision of two bubbles. Our problem is highly relativistic—the velocity of the bubble walls asymptotically approaches the speed of light as the bubbles expand—but gravity plays a negligible role—the bubble expansion is driven by the pressure difference between the true and false vacua.

Throughout the present calculation, we make the following assumptions:

1. Gravity is linearized, and gravitational effects on the expansion of the bubble itself are neglected. The radiation produced by the gravitational field of the bubbles and back reaction of radiation on the bubble motion are of course also ignored. In this approximation the gravitational radiation problem is precisely analogous to its electromagnetic counterpart (except for additional tensor structure).
2. Since the source reaches velocities very close to the speed of light, it is necessary to keep many terms in the source velocity v/c. We keep all orders in v/c, although a self-consistent approximation dictates expanding only to order n in the velocity, where $\phi/c^2 \sim (v/c)^n$. This approximation is commonly known as the "post-Minkowski" or "linearized" wave-generation formalism.
3. The source is localized in space, so it is possible to define a "far-field zone" and use standard radiation formalism. A pair of vacuum bubbles expanding indefinitely is not a localized source, but because we impose a time cutoff (as explained above), the source for our problem is localized.
4. We ignore the expansion of the Universe and gravitational effects on bubble nucleation. In the limit that the cutoff time τ is much less than te Hubble time H^{-1} this is a valid approximation; as we shall see in Sec. VI, one expects $\tau \lesssim H^{-1}$.

Before going on let us estimate the gravitational potential associated with the bubble.

Just outside a bubble of radius R, the gravitational potential is $\phi \sim R^3\rho_{\rm vac}/R \sim (R/H^{-1})^2$. Thus we see that $\phi/c^2 \lesssim v^2/c^2 \sim \mathcal{O}(1)$ provided that the radius of the bubble is less than the Hubble length, H^{-1}; since the radius of the bubble $R \simeq t \leq \tau$ neglecting the gravitational effects is justified so long as $\tau \lesssim H^{-1}$. The condition $\phi/c^2 \lesssim v^2/c^2$ justifies neglecting gravitational effects on the expansion of the bubble as well. Finally, recall that the initial size of the bubble relative to the Hubble radius, $R_0/H^{-1} \sim \varphi_0/m_{\rm Pl}$, is expected to be very small, provided that $\varphi_0 \ll m_{\rm Pl}$.

(b) Gravitational radiation in the linearized approximation

Now we write down the formalism for computing gravitational radiation from a source in the linearized-gravity approximation. All necessary information is contained in the space-space components of its stress-energy tensor $T^{\mu\nu}(\mathbf{x},t)$; we follow the treatment given by Weinberg [18]. He defines the space-space components of the Fourier-transformed stress tensor with the unusual convention

$$T_{ij}(\hat{\mathbf{k}},\omega) = \frac{1}{2\pi}\int dt e^{i\omega t}\int d^3x T_{ij}(\mathbf{x},t)e^{-i\mathbf{k}\cdot\mathbf{x}}. \tag{16}$$

The components contributing to gravitational radiation satisfy the null condition $k_\mu k^\mu = 0$, *i.e.*, $|\mathbf{k}| = \omega$. The total energy radiated in the direction $\hat{\mathbf{k}}$ into the solid angle $d\Omega$ at frequency ω is given by

$$\frac{dE}{d\omega d\Omega} = 2G\omega^2\Lambda_{ij,lm}(\hat{\mathbf{k}})T^{ij*}(\mathbf{k},\omega)T^{lm}(\mathbf{k},\omega), \tag{17}$$

where $\Lambda_{ij,lm}$ is the projection tensor for gravitational radiation,

$$\begin{aligned}\Lambda_{ij,lm}(\hat{\mathbf{k}}) \equiv \delta_{il}\delta_{jm} - 2\hat{\mathbf{k}}_j\hat{\mathbf{k}}_m\delta_{il} + \frac{1}{2}\hat{\mathbf{k}}_i\hat{\mathbf{k}}_j\hat{\mathbf{k}}_l\hat{\mathbf{k}}_m \\ - \frac{1}{2}\delta_{ij}\delta_{lm} + \frac{1}{2}\delta_{ij}\hat{\mathbf{k}}_l\hat{\mathbf{k}}_m + \frac{1}{2}\delta_{lm}\hat{\mathbf{k}}_i\hat{\mathbf{k}}_j.\end{aligned} \tag{18}$$

Our problem is axially symmetric about the z-axis connecting the two bubble centers, so without loss of generality we can take

$$\hat{\mathbf{k}}_x = \sin\theta, \qquad \hat{\mathbf{k}}_y = 0, \qquad \hat{\mathbf{k}}_z = \cos\theta \tag{19a}$$

$$\mathbf{k} = \omega\hat{\mathbf{k}}; \qquad \omega_x \equiv \omega\sin\theta, \qquad \omega_z \equiv \omega\cos\theta. \tag{19b}$$

We note the following symmetry properties of the projection tensor:

$$\Lambda_{ij,lm} = \Lambda_{lm,ij}\,; \tag{20a}$$

$$\Lambda_{ij,lm}\delta_{ij} = 0\,; \tag{20b}$$

$$\Lambda_{ij,lm}\hat{\mathbf{k}}_i\hat{\mathbf{k}}_j = 0\,; \tag{20c}$$

$$\Lambda_{ij,lm}\delta_{iz}\delta_{jz}\delta_{lz}\delta_{mz} = \Lambda_{zz,zz} = \frac{1}{2}(1-\hat{\mathbf{k}}_z{}^2)^2 = \frac{1}{2}\sin^4\theta. \tag{20d}$$

For the stress-energy tensor we take the canonical form

$$T_{\mu\nu} = \partial_\mu\varphi\,\partial_\nu\varphi - \mathcal{L}g^{\mu\nu}. \tag{21}$$

From Eqs. (17) and (20b), it follows that any term in $T_{ij}(k)$ proportional to δ_{ij} yields no gravitational radiation ("pure trace" terms do not contribute to gravitational radiation). Thus for the purposes of calculating radiation, we make the replacement

$$T_{ij}(\mathbf{x},t) = \partial_i\varphi\,\partial_j\varphi + \delta_{ij}\mathcal{L} \longrightarrow \partial_i\varphi\,\partial_j\varphi. \tag{22}$$

From this point on, all references to T_{ij} actually mean $\partial_i\varphi\partial_j\varphi$.

(c) Quadrupole approximation

Before exhibiting the components of the Fourier-transformed stress tensor in full generality, we consider quadrupole approximation. The familiar quadrupole approximation is obtained simply by taking the limit $\mathbf{k}\cdot\mathbf{x} \to 0$:

$$\begin{aligned} T_{ij}(\hat{\mathbf{k}},\omega) \longrightarrow T^Q_{ij}(\omega) &\equiv \frac{1}{2\pi}\int dt\, e^{i\omega t}\int d^3x\, T_{ij}(\mathbf{x},t) \\ &= \int dt\, e^{i\omega t}\int d^3x\,\partial_i\varphi\,\partial_j\varphi. \end{aligned} \tag{23}$$

With axial symmetry about the z-axis, the off-diagonal components are zero and $T^Q_{ij}(\omega)$ must be of the form

$$T^Q_{ij}(\omega) = D(\omega)\delta_{ij} + \Delta(\omega)\delta_{iz}\delta_{jz}. \tag{24}$$

Further, the first term does not contribute to gravitational radiation. The second term is given by

$$\begin{aligned} \Delta(\omega) &= T^Q_{zz} - \frac{1}{2}(T^Q_{xx} + T^Q_{yy}) \\ &= \frac{1}{2\pi}\int_0^\infty dt\, e^{i\omega t}\int d^3x\left[\left(\frac{\partial\varphi}{\partial z}\right)^2 - \frac{1}{2}\left(\frac{\partial\varphi}{\partial x}\right)^2 - \frac{1}{2}\left(\frac{\partial\varphi}{\partial y}\right)^2\right] C(t) \\ &= \int_0^\infty dt\, e^{i\omega t}\int_{-\infty}^\infty dz\int_0^\infty r\,dr\left[\left(\frac{\partial\varphi}{\partial z}\right)^2 - \frac{1}{2}\left(\frac{\partial\varphi}{\partial r}\right)^2\right] C(t), \end{aligned} \tag{25}$$

where $C(t)$ is the time cutoff discussed in the previous Section, cf. Eq. (11), and r is the radial polar coordinate in the $x-y$ plane. Note also that we have assumed the nucleation events take place at $t = 0$.

If the two bubbles are nucleated simultaneously, the field is a function only of the two variables s and z; a further change of variables to the hyperbolic coordinates

$$t = s\cosh\psi, \quad r = s\sinh\psi, \quad u = \cosh\psi \qquad (t^2 > r^2) \tag{26a}$$

$$t = s\sinh\psi, \quad r = s\cosh\psi, \quad u = \sinh\psi \qquad (t^2 < r^2) \tag{26b}$$

leads to the following expressions:

$$r^2 < t^2: \quad \Delta_1(\omega) = \int_0^\infty s^2\,ds \int_{-\infty}^\infty dz \Big(\frac{\partial\varphi}{\partial z}\Big)^2 \int_1^\infty du\, e^{i\omega s u}\, C(su)$$
$$- \frac{1}{2}\int_0^\infty s^2\,ds \int_{-\infty}^\infty dz \Big(\frac{\partial\varphi}{\partial s}\Big)^2 \int_1^\infty du\,(u^2-1) e^{i\omega s u}\, C(su); \quad (27a)$$

$$r^2 > t^2: \quad \Delta_2(\omega) = \int_0^\infty s^2\,ds \int_{-\infty}^\infty dz \Big(\frac{\partial\varphi}{\partial z}\Big)^2 \int_0^\infty du\, e^{i\omega s u}\, C(su)$$
$$- \frac{1}{2}\int_0^\infty s^2\,ds \int_{-\infty}^\infty dz \Big(\frac{\partial\varphi}{\partial s}\Big)^2 \int_0^\infty du\,(u^2+1) e^{i\omega s u}\, C(su); \quad (27b)$$

$$\Delta(\omega) = \Delta_1(\omega) + \Delta_2(\omega). \quad (27c)$$

The subscripts "1" and "2" denote the two regions of integration. Note that functions of φ depend only upon s and z. By using equation (20d), it follows that in the quadrupole approximation

$$\frac{dE}{d\omega d\Omega} = G\omega^2 |\Delta(\omega)|^2 \sin^4\theta \quad (28)$$

where, as before, $\hat{\mathbf{k}}_z = \cos\theta$.

The quadrupole approximation is of interest because it is much simpler numerically than the full, linearized-gravity approximation. It also provides a check on our numerical results, since the radiation in the quadrupole approximation and the full, linearized-gravity calculation must have the same asymptotic behavior in the limit that $\omega \to 0$. We do not, however, expect the quadrupole approximation to be accurate because our expanding bubbles are highly relativistic. In fact, we would naively expect the quadrupole approximation to *underestimate* the amount of gravitational radiation in our problem. As we shall see, quite the opposite is true: the total energy radiated in the quadrupole approximation is more than a factor of 50 larger than that in the full, linearized-gravity calculation, which includes all the multipoles [19]! Since the total energy radiated in the linearized approximation is presumably an incoherent sum of all the multipoles, this presents a paradox of sorts. We will return to this point later (its resolution is explained in Appendix B).

(d) Full, linearized-gravity approximation

Fixing $\hat{\mathbf{k}}_y = 0$ with the given axial symmetry implies $T^{xy}(\hat{\mathbf{k}},\omega) = T^{yz}(\hat{\mathbf{k}},\omega) = 0$. The procedure for calculating the remaining components of $T^{ij}(\hat{\mathbf{k}},\omega)$ is straightforward and essentially the same as in the quadrupole case, with the additional factor of $e^{-i\mathbf{k}\cdot\mathbf{x}}$ in the integrand:

$$T_{ij}(\hat{\mathbf{k}},\omega) = \frac{1}{2\pi}\int_0^\infty dt\, e^{i\omega t} \int d^3x\, e^{-i\mathbf{k}\cdot\mathbf{x}} \partial_i\varphi\partial_j\varphi. \quad (29)$$

The polar-coordinate transformation gives, *e.g.*,

$$T^{xx}(\hat{\mathbf{k}},\omega) = \frac{1}{2\pi}\int_0^\infty dt\, e^{i\omega t}\int_{-\infty}^{\infty} dz \int_{-\pi}^{\pi} d\eta \int_0^\infty r dr \left(\frac{\partial\varphi}{\partial r}\right)^2 \cos^2\eta e^{-i\omega_x r\cos\eta - i\omega_z z}. \quad (30)$$

The η integral can be performed explicitly using the Bessel-function identity

$$\int_{-\pi}^{\pi} e^{i\beta\cos x}\cos nx\, dx = 2i^n\pi J_n(\beta). \quad (31)$$

Then, for the equal-bubble case, the same hyperbolic-coordinate transformations yield various expressions of the form

$$T_1^{xx}(\hat{\mathbf{k}},\omega) = \frac{1}{2}\int_0^\infty s^2\, ds \int_{-\infty}^{\infty} dz\, e^{i\omega_z z}\left(\frac{\partial\varphi}{\partial s}\right)^2 \int_1^\infty du(u^2-1)e^{i\omega s u} \times \left[J_0(\omega_x s\sqrt{u^2-1}) - J_2(\omega_x s\sqrt{u^2-1})\right] C(su).$$

The complete expressions for $T^{ij}(\hat{\mathbf{k}},\omega)$ are given in Appendix A. The required contraction with the projection tensor, cf. Eq. (17), can be reduced to

$$\frac{dE}{d\omega d\Omega} = G\omega^2\Big[T^{zz}(\hat{\mathbf{k}},\omega)\sin^2\theta + T^{xx}(\hat{\mathbf{k}},\omega)\cos^2\theta - T^{yy}(\hat{\mathbf{k}},\omega) - 2T^{xz}(\hat{\mathbf{k}},\omega)\sin\theta\cos\theta\Big]^2. \quad (32)$$

(e) Unequal bubbles

For two bubbles nucleated at different times, the situation is more complicated, as the field is no longer a function only of the two variables s and z. In principle, the evolution of the field φ is now three dimensional (two space and one time), making the problem computationally intractable. However, if two bubbles are nucleated at different times with a space-like interval between the nucleation events, there is an appropriate Lorentz boost to a frame in which the bubbles are nucleated simultaneously. The formulae derived in Section III(d) are valid in the boosted frame, except for the time cutoff. In the original unequal-bubble frame, the cutoff is spatially uniform; in the boosted frame the cutoff is dependent on both time and space. We can use the equations derived above for the unequal bubble case, provided that the cutoff function $C(t)$ is replaced by the "tilted" cutoff function $C[\gamma(t+\beta z)]$. For unequal bubbles, we calculate the resulting radiation by: (a) transforming to the frame in which the nucleation times are equal; (b) using the formalism of Section III(d), modified by the tilted cutoff, to calculate the radiation spectrum; and (c) transforming the spectrum of gravitational radiation back to the original frame.

IV. Naive Expectations and Scalings

As is often the case, the dynamical range accessible to numerical techniques does not allow exploration of the full range of parameter space. Therefore, it is very important to discover any exact or approximate scaling relations that exist. The present problem possesses several useful scaling relations that can be anticipated—and verified by our numerical work. The problem of two colliding vacuum bubbles has several time/length scales: the separation of the bubbles d; the cutoff time τ, which, since the bubbles expand at essentially the speed of light, sets the bubble size at the cutoff; the initial bubble size, $R_0 \simeq 1/\sqrt{\lambda}\epsilon\varphi_0$; and the initial thickness of the bubble wall, ΔR, also of order φ_0^{-1}. In the context of a phase transition, τ corresponds to the duration of the transition, and as we shall discuss in Section VI, the duration of the transition and the bubble separation are expected to be of the same order: $d \sim \tau$. Further, τ is expected to be of order $few \times 10^{-2}H^{-1}$, which implies that $d, \tau \gg R_0$, the initial bubble size. This makes R_0 an irrelevant length scale. Finally, there is the bubble-wall thickness, ΔR, which is initially of order R_0, but which decreases with time due to Lorentz contraction. *A priori,* the bubble-wall thickness could be an important scale; as we shall see it is not. In the end, for the case of two colliding vacuum bubbles of equal size there is but one relevant time/length scale: τ.

Let us now estimate the gravitational radiation produced by the collision of two bubbles. Recall that in the quadrupole approximation, the power emitted in gravitational waves is given by

$$P_{\rm GW} \sim G Q_3^2; \tag{33a}$$

$$E_{\rm GW} \sim G \int Q_3(t)^2 dt \sim \int Q_3(\omega)^2 d\omega; \tag{33b}$$

where Q is the quadrupole moment of the energy distribution, $Q_3(t) \equiv d^3Q/dt^3$, and $Q_3(\omega) \sim \int Q_3(t) \exp(i\omega t)$ is the Fourier transform of the triple-time derivative of the quadrupole moment. Assuming, as we have, that τ is the only relevant time/length scale, $Q_3 \sim \rho_{\rm vac}\tau^2$, where $\rho_{\rm vac}$ is the energy density associated with the false-vacuum state. It now follows that

$$E_{\rm GW} \sim G\rho_{\rm vac}^2\tau^5; \qquad Q_3(t) \sim \tau^2 f(t/\tau);$$
$$Q_3(\omega) \sim \tau^3 f(\omega\tau); \qquad dE_{\rm GW}/d\omega \sim \tau^6 |f(\omega\tau)|^2; \tag{34}$$

where the function f does not depend upon τ.

Expressions (34) contain the essence of our expectations for scaling behavior: (i) First, the energy emitted in gravity waves depends upon the size of the bubbles when they collide to the fifth power; (ii) The spectrum of gravitational waves is an invariant function of $\omega\tau$, so that the characteristic frequency of radiation varies as τ^{-1}; and (iii) $dE_{\rm GW}/d\omega$ varies as $\rho_{\rm vac}^2\tau^6$. As we shall see, all of these scalings are verified numerically. In a highly relativistic problem, one might question whether scalings based upon the quadrupole approximation bear up when the full, relativistic calculation is done. The answer is yes, basically because these relations follow from dimensional considerations.

The most crucial point is that the energy emitted in gravitational waves varies as the fifth power of the separation of the nucleated bubbles. The absolute energy radiated in gravitational waves is of less interest than the fraction of the vacuum energy liberated into gravitational waves. The false-vacuum energy released scales as

$$E_{\rm vac} \sim \rho_{\rm vac} \tau^3. \tag{35}$$

Comparing this to the energy radiated in gravity waves gives

$$f \equiv \frac{E_{\rm GW}}{E_{\rm vac}} \sim \frac{G\rho_{\rm vac}^2 \tau^5}{\rho_{\rm vac}\tau^3} \sim \frac{\tau^2}{(G\rho_{\rm vac})^{-1}} \sim \left(\frac{\tau}{H^{-1}}\right)^2. \tag{36}$$

That is, the energy fraction liberated into gravity waves varies as τ^2; further we recognize $\sqrt{G\rho_{\rm vac}}$ as the Hubble parameter associated with the expansion of the Universe driven by the false-vacuum energy density. Thus, we discover the fundamental relation that f is proportional to the square of the size of the typical bubbles when they collide relative to the Hubble radius [10]. Since the false-vacuum energy liberated by bubble collisions is responsible for "reheating" the Universe in extended inflation (or in a strongly first-order phase transition in which the entropy of the Universe is greatly increased), the ratio of energy density in gravitational waves to radiation after the transition is also f.

Finally, what are our expectations for the gravitational radiation produced by the collision of bubbles of unequal size? Suppose at the time of collision (*i.e.*, when the two bubbles first "kiss") the larger bubble has size R and the smaller bubble size r ($\ll R$). Since we expect the smaller bubble to be encompassed by the larger bubble in a time of order r, the time cutoff will also be of order r. The controlling time/length scale in this problem is r: The size of the collision region will be characterized by r, and the time rate of change of the quadrupole distortion will occur on the time scale r. (We of course assume that at collision, both bubbles are much larger than their initial sizes.) As in the equal bubble case, the relevant time/length scale determines the scaling relations:

$$E_{\rm GW} \sim G\rho_{\rm vac}^2 r^5, \qquad \frac{dE_{\rm GW}}{d\omega} \sim G\rho_{\rm vac}^2 r^6, \qquad \omega \sim r^{-1}, \tag{37}$$

and

$$f \equiv \frac{E_{\rm GW}}{E_{\rm vac}} \sim G\rho_{\rm vac} r^2 \sim \left(\frac{r}{H^{-1}}\right)^2. \tag{38}$$

Note that expressions (37) and (38) only depend upon the size of the small bubble, and have the same form as the corresponding expressions in the "equal-bubble" case—and thus smoothly extrapolate to the case $R = r \sim \tau$. The lack of dependence upon R follows because the scale r controls all the action—the size of the quadrupole moment and its time variation. As we shall discuss in the final Section, we do not expect a great disparity in bubble sizes: in a typical first-order transition, the distribution of bubble sizes is gaussian with a width that is about half the mean bubble size.

As we shall now discuss, our numerical results bear out the scaling expectations discussed here; in particular, that $dE_{\rm GW}/d\omega \propto {\rho_{\rm vac}}^2\tau^6$, and that $f \simeq 1.3\times 10^{-3}(\tau/H^{-1})^2$. As stated at the beginning of this Section the discovery of these scalings is crucial to applying our results to realistic situations. To illustrate, consider the following example. In our largest simulation, $\tau \sim 100R_0 \sim 10^3/\sqrt{\lambda}\varphi_0$. For a realistic phase transition we expect $\tau \sim few \times 10^{-2}H^{-1} \sim 10^{-2}m_{\rm Pl}/\sqrt{\lambda}\varphi_0^2 \sim 10^{-2}(m_{\rm Pl}/\varphi_0)R_0$. For $\varphi_0 \sim 10^{15}\,{\rm GeV}$, our simulation is just large enough to handle the realistic scenario; for $\varphi_0 \ll 10^{15}\,{\rm GeV}$, our simulation is far too small. However, because the results scale, we can make reliable estimates even for $\varphi_0 \ll 10^{15}\,{\rm GeV}$.

V. Numerical Considerations and Results

Expressions (27a-b) and (A1-A8) for the various components of $T^{ij}(\hat{\mathbf{k}},\omega)$ needed to compute $dE/d\omega d\Omega$ are complicated integrals over the scalar field $\varphi(\mathbf{x},t)$. As such they cannot be evaluated in closed form, so we must resort to numerical techniques to evaluate them. The numerical work consists of two parts: evolving the field and evaluating the integrals. We work with dimensionless units, defined in terms of the scales associated with the scalar field φ. The mass of the scalar field $m_\varphi^2 = \lambda\varphi_0^2$ defines the natural time/length scale: $m_\varphi^{-1} = \lambda^{-1/2}\varphi_0^{-1}$; and $\lambda\varphi_0^4$ defines the natural scale for energy density. We thus define the dimensionless quantities, denoted by a tilde:

$$(x,t) = (\tilde{x},\tilde{t})\lambda^{-1/2}\varphi_0^{-1}; \qquad (\omega,k) = (\tilde{\omega},\tilde{k})\lambda^{1/2}\varphi_0; \qquad \varphi = \tilde{\varphi}\varphi_0; \tag{39}$$

where (x,t) are (length, time), (ω,k) are (frequency, wavenumber), ρ is energy density, and of course $\hbar = c = 1$. The Lagrangian density becomes

$$\mathcal{L} = \lambda\varphi_0^4\left[\frac{1}{2}\frac{\partial\tilde{\varphi}}{\partial\tilde{x}^\mu}\frac{\partial\tilde{\varphi}}{\partial\tilde{x}_\mu} - \frac{1}{8}(\tilde{\varphi}^2-1)^2 - \epsilon(\tilde{\varphi}+1)\right]. \tag{40}$$

In terms of these dimensionless units, the quantities that we calculate are related to physical units by

$$\frac{dE_{\rm GW}}{d\omega} = \lambda^{-1}\left(\frac{\varphi_0}{m_{\rm Pl}}\right)^2\frac{d\tilde{E}_{\rm GW}(\epsilon)}{d\tilde{\omega}}; \tag{41a}$$

$$\frac{dE_{\rm GW}}{d\omega}\tau^6 = \lambda^{-4}\varphi_0^{-4}{m_{\rm Pl}}^{-2}\frac{d\tilde{E}_{\rm GW}(\epsilon)}{d\tilde{\omega}}\tilde{\tau}^6; \tag{41b}$$

$$E_{\rm GW}(\epsilon) = \lambda^{-1/2}\frac{\varphi_0^3}{{m_{\rm Pl}}^2}\tilde{E}_{\rm GW}(\epsilon); \tag{41c}$$

$$\rho_{\rm vac} = \lambda\varphi_0^4\tilde{\rho}_{\rm vac}. \tag{41d}$$

Note that the dimensionless units for the quantities involving $E_{\rm GW}$ differ by a factor of $\varphi_0^2/{m_{\rm Pl}}^2$ from other energy-related quantities (due to the dimensional factor of Newton's constant $G = {m_{\rm Pl}}^{-2}$ in their definitions). While the dimensionless quantities $d\tilde{E}_{\rm GW}/d\tilde{\omega}$

and $\tilde{E}_{\rm GW}$ are independent of λ, they do depend upon ϵ, scaling as ϵ^2 (which follows from the fact that $E_{\rm GW} \propto \rho_{\rm vac}^2$). In all of the results and Figures that follow, we use dimensionless units but omit the tildes for ease of notation. To recover the physical units of dimensionless quantities, simply use the conversion factors given above.

(a) Field evolution

As mentioned above, for the case of two bubbles nucleated simultaneously, the wave equation governing the field evolution can be converted to a 1+1 dimensional partial-differential equation in the space coordinate z and the "time" coordinate s. First, Eqs. (4) and (5) are solved for the bubble profile using a straightforward estimator method. The initial conditions are the field values along the z-axis connecting the two bubbles; for the equal bubble case, we have reflection symmetry about the $z = 0$ plane, so only the field values for $z \geq 0$ must be calculated. We impose a reflective boundary condition at $z = 0$ and evolve the field in steps using Eq. (15) with a staggered leapfrog algorithm. Recall that the bubble-wall thickness decreases roughly as t^{-1} due to Lorentz contraction; our step size is chosen to give reasonable resolution of the final bubble wall-thickness (at least ten grid points across the thickness of the bubble wall).

A common check on the accuracy of scalar field evolution is to calculate the total energy of the field at each time step and make sure energy is conserved to within some prescribed tolerance. Unfortunately, since the "time" variable s is not the true time (recall $s^2 = t^2 - r^2$) energy is not conserved from one s-step to the next. But the energy between s-steps does change in a definite way, and we can use this fact as a check on the scalar-field evolution [16]. The Hamiltonian density of the field is

$$\mathcal{H}(s,z) = \frac{1}{2}\Big(\frac{\partial\varphi}{\partial s}\Big)^2 + \frac{1}{2}\Big(\frac{\partial\varphi}{\partial z}\Big)^2 + V(\varphi). \tag{42}$$

Consider an infinitesimally thin tube of radius dr along the z-axis; the total energy contained in this tube is

$$\begin{aligned} E(t)dr &= 2\pi dr\Big[\int_{-\infty}^{\infty} dz\,\mathcal{H}(z,r,t)\Big]\Big|_{r=0} \\ &= 2\pi dr\int_{-\infty}^{\infty} dz\,\Big(\frac{1}{2}\Big(\frac{\partial\varphi}{\partial s}\Big)^2 + \frac{1}{2}\Big(\frac{\partial\varphi}{\partial z}\Big)^2 + V(\varphi)\Big)\Big|_{s=t} \end{aligned} \tag{43}$$

Taking the time derivative (equivalently, the s-derivative) of both sides gives

$$\begin{aligned} \frac{dE(s)}{ds} &= 2\pi\int_{-\infty}^{\infty} dz\,\Big(\frac{\partial^2\varphi}{\partial s^2}\frac{\partial\varphi}{\partial s} + \frac{1}{2}\frac{d}{ds}\Big(\frac{\partial\varphi}{\partial z}\Big)^2 + \frac{\partial V}{\partial\varphi}\frac{\partial\varphi}{\partial s}\Big) \\ &= 2\pi\int_{-\infty}^{\infty} dz\,\Big(\frac{\partial\varphi}{\partial s}\Big)\Big(\frac{\partial^2\varphi}{\partial s^2} - \frac{\partial^2\varphi}{\partial z^2} + \frac{\partial V}{\partial\varphi}\Big) \\ &= -\frac{4\pi}{s}\int_{-\infty}^{\infty} dz\,\Big(\frac{\partial\varphi}{\partial s}\Big)^2 \end{aligned} \tag{44}$$

where we have integrated by parts and the used the equation of motion, Eq. (15). As a field-evolution check, at each s-step we calculate the total energy, Eq. (43), as well as an estimate by integrating Eq. (44) over all the s-steps to that point, and make sure the two match to within a given error, which we generally take to be 2% for all times. We choose our s- and z-partition sizes to be 0.025 and 0.05, which gives acceptable field evolution for all but our largest bubble separation; for $d = 480$ the energy check has an error of around 7% at the time cutoff. Note the initial bubble size in dimensionless units is $R_0 \sim 10$. For the largest simulations, taking a finer grid spacing actually increases the error in the field evolution, suggesting that our precision is limited by accumulated roundoff errors and not by partition size. We believe that this inaccuracy in the field evolution does not significantly affect our calculations.

(b) Numerical integration

Formulas (A1-A8) must be evaluated to compute the amount of gravitational radiation from two bubbles nucleated simultaneously. The task at hand is to evaluate numerically a three-dimensional integral, for many values of $\hat{\mathbf{k}}$ (direction) and ω. Reflection symmetry reduces the range of z-integration to positive values. Note that for a given value of s, the z-integral and the u-integral are independent, since the field derivatives depend only upon s and z. In effect, the integrals are each a pair of double integrals instead of a single triple integral. This greatly aids numerical evaluation. First we choose values for ω, the frequency of the radiated power, and θ, the polar angle of the direction of radiation ($\hat{\mathbf{k}}_z = \cos\theta$). Then beginning with the initial bounce solution for $\varphi(z)$, we evolve the field with the "time" variable s. After a certain number of time steps, we evaluate the z-integral with a Simpson's Rule integration over the partition of φ, and the u-integral with a trapezoidal integration over a partition which varies in size depending upon how many oscillations of the integrand occur in the region of integration. These two integrals are multiplied together, and a running sum for the s-integral is incremented. Note that the z and u integrals are not true Fourier transforms, since the transform variable ω appears in the integrand as well as in the exponential factor. Thus the usual technique of the Fast Fourier Transform cannot be used.

We have tested our code in a variety of ways. First we have computed the gravitational radiation from a single, expanding bubble; while not precisely zero, it is about seven orders of magnitude smaller than that from two colliding bubbles. We have also computed the amount of radiation when the cutoff τ is less than $d/2$, so that the two vacuum bubbles do not collide. Again, the result is seven orders of magnitude smaller than in the case of two colliding bubbles. Finally, the asymptotic behavior of the full linear result and the quadrupole result are identical as $\omega \to 0$.

As explained in Section III(e), the case of two bubbles nucleated at different times is equivalent to the equal-bubble case with a tilted time cutoff $C(t, z)$. In the expressions for the stress-tensor components, the z-integral and the u-integral, which are independent

in the equal-bubble case, are now coupled since the u-integrand depends explicitly on z through the cutoff function $C(su, z)$. This of course makes the numerical evaluation of the integrals much more time consuming, since now we must evaluate triple integrals. We are limited to only a handful of data points for unequal bubbles, as the computing time involved is nearly two orders of magnitude greater than in the equal-bubble case.

(c) Results for equal bubbles

We consider identical bubbles nucleated at time $t = 0$ with centers on the z-axis at $z = \pm d/2$. A geometrical criterion for the cutoff time τ is used:

$$\tau = \sqrt{(\alpha d)^2 - R_0^2} \approx \alpha d; \tag{45}$$

that is, at the cutoff time, the bubble radii are αd (disregarding bubble interactions). This is geometrical in the sense that for any value of d, the bubble configuration at $t = \tau$ will look identical, up to an overall rescaling of distance. The final bubble configuration for representative values of α is shown schematically in Fig. 3.

We begin with the results for our "benchmark case": initial separation $d = 60$; cutoff time factor $\alpha = 1.2$; cutoff function given by Eq. (11) with $\tau_c = 0.9\tau$ and $\tau_0 = 4(\tau - \tau_c)$; scalar-field potential given by Eq. (2) with $\epsilon = 0.1$. In dimensionless units, for $\epsilon = 0.1$, the initial bubble radius is $R_0 \approx 9.5$, making the cutoff time $\tau = 71.37$. After discussing the results for this case, we vary the parameters individually and explore how the results change. For each case, we calculate $dE_{\rm GW}/d\omega d\Omega$ for a range of frequencies, at angular increments of 2°. The energy spectrum $dE/d\omega$ is obtained by a numerical integration of $dE/d\omega d\Omega$ over solid angle.

Figures 4a and 4b show radiation patterns for the benchmark case, *i.e.*, polar plots of $dE/d\Omega d\omega$ for $0 \leq \theta \leq \pi$ for various values of ω. Recall that the problem possesses axial symmetry, so the energy radiated into the solid angle $d\Omega$ is independent of the azimuthal angle ϕ. Further, symmetry dictates that $dE/d\omega d\Omega$ vanish along the z-axis. As the frequency approaches zero, the radiation pattern approaches the quadrupole pattern. As the frequency increases, higher multipoles dominate and the "antenna pattern" develops more and more lobes. In Fig. 5 we display the integrated radiation pattern, $dE/d\Omega$. Superimposed is an unnormalized quadrupole pattern for comparison. Clearly higher multipoles make a significant contribution to the total energy radiated.

The substantial power from higher multipoles would suggest that the quadrupole approximation should not be very good for this problem—as expected since the problem is highly relativistic. This is the case: Fig. 6 shows $dE/d\omega$ in the quadrupole approximation and in the full-linearized approximation ("all multipoles"); however, the radiation from the quadrupole calculation is much greater than the radiation from the full calculation! This is paradoxical since the full calculation is just an incoherent sum of all the multipoles, and thus must be greater than the quadrupole contribution. We discuss in detail the resolution to this paradox in Appendix B. Briefly, the explanation is that the familiar "quadrupole

approximation" is not precisely the quadrupole multipole that appears in the multipole expansion. An additional assumption has been made in deriving the "quadrupole approximation," namely that the source is small, having physical size $\ll \omega^{-1}$. In nonrelativistic systems this condition is satisfied, since the physical size is set by a characteristic velocity times ω^{-1}. The "exact quadrupole"—computed without assuming that the source is small—is indeed smaller than the sum of all the multipoles. A simple analytic model considered at the end of Appendix B nicely reproduces the ratio between our quadrupole approximation and full-linearized calculation.

Fig. 7 illustrates the principal result of this paper. We vary d while holding other parameters fixed; in particular $\alpha = 1.2$, so that $\tau = 1.2d$. In Fig. 6 the scaled energy spectrum, $\tau^{-6} dE_{\rm GW}/d\omega$, is shown as a function of $\omega\tau$. According to our naive expectations, $\tau^{-6} dE_{\rm GW}/d\omega$ should only be a function of $\omega\tau$: the spectrum for all values of τ should coincide. This is the case; the spectra for τ=192, 288, 360, and 576 are virtually indistinguishable. The spectra for τ=120 and 72 differ from these by about 20% and 80% respectively. Note that in going from $\tau = 72$ to $\tau = 576$, $dE_{\rm GW}/d\omega$ has increased by a factor of about 3×10^5!

The approach to scaling as τ becomes very large is quite convincing. The relatively large discrepancy for $\tau = 72$ ($d = 60$) is easily understood: in this case the initial bubble size, $R_0 \simeq 10$, is not negligible compared to the final bubble size, $R \approx 72$, and the neglect of the initial bubble size is not as well justified. In any case, scaling is quite apparent in the regime of relevance, $\tau \sim d \gg R_0$. If we integrate the spectrum over frequency (in the scaling regime), we find that

$$E_{\rm GW} \simeq 1.7 \times 10^{-3} \tau^5,$$

in our dimensionless units (and for $\epsilon = 0.1$).

In Fig. 8 we show the spectrum in the scaling regime plotted slightly differently: $\tau^{-6} dE_{\rm GW}/d\ln\omega\tau$ as a function of $\omega\tau$. This corresponds to the energy radiated per octave, and we note that $dE_{\rm GW}/d\ln\omega\tau$: (i) peaks at a frequency $\omega_{\rm max} \simeq 3.8/\tau$; (ii) increases as $(\omega\tau)^{2.8}$ for $\omega \lesssim \omega_{\rm max}$; and (iii) decreases as $(\omega\tau)^{-1.8}$ for $\omega \gtrsim \omega_{\rm max}$. That is, the energy radiated in gravitational waves has a characteristic frequency: $\omega_{\rm max} \simeq 3.8/\tau$.

Now consider the scaling with τ for fixed d, under variations of α. For a realistic phase transition, we expect d to be of the order of τ; *i.e.*, duration of the phase transition comparable to the initial bubble separation (see Sec. VI). In Fig. 9 we show the total energy radiated as a function of α for $d = 60$ fixed, with α ranging from 1 to 8. This range of α corresponds to the phase transition ending when each bubble wall just reaches the other bubble's center ($\alpha = 1$), to it ending when each bubble wall has moved a factor of 8 times the distance to the other bubble's center. Over the range $\alpha \simeq 1$ to 2 or so, $E_{\rm GW} \propto \alpha^5$, as expected from the scaling prediction $dE_{\rm GW}/d\omega \propto \tau^6$ (valid for $d \sim \tau$). For the largest values of α, $E_{\rm GW}$ increases more slowly than this, and we expect that in the unphysical limit $\alpha \gg 1$, $E_{\rm GW} \propto \alpha^3$ [20]. To recapitulate, by varying both α and d, we have

shown that, provided $d \sim \tau$ (*i.e.*, α of order unity), the energy spectrum $\tau^{-6} dE_{\rm GW}/d\omega$ is only a function of $\omega\tau$, and the total energy radiated in gravity waves $E_{\rm GW} \propto \tau^5$. (That is, neither quantity explicitly depends upon d or α, provided $\alpha \sim \mathcal{O}(1)$ and $d \gg R_0$.)

Next, consider the scaling of the energy radiated in gravity waves with the vacuum-energy density; in the previous Section we argued that $E_{\rm GW} \propto \rho_{\rm vac}^2$. To vary $\rho_{\rm vac}$ we have varied ϵ (from 0.033 to 0.15); recall that for the potential given by Eq. (2), $\rho_{\rm vac} = 2\epsilon\lambda\varphi_0^4$ is a good approximation. Changing ϵ not only changes $\rho_{\rm vac}$, but also changes the initial size of the bubble, R_0, and the shape and thickness of the bubble wall. In Fig. 10 we show $E_{\rm GW}$ as a function of $\rho_{\rm vac}$, for $d = 240$ and $\alpha = 1.2$; it is apparent that $\rho_{\rm GW}$ scales quite precisely as $\rho_{\rm vac}^2$. As a further test of this scaling we have also tried an alternative form for the scalar potential,

$$V(\varphi) = \frac{\lambda}{8}(\varphi^2 - \varphi_0^2)^2 + \epsilon\lambda\varphi_0(\varphi^3 - \varphi_0^3); \tag{46}$$

where the term that the breaks the degeneracy between the two vacua is cubic rather than linear. The energy radiated in gravity waves in this case falls neatly on the same line as for our original potential.

Finally, recall that we introduced a time cutoff τ to take into account the fact that the vacuum bubbles do not expand into the false vacuum forever; eventually they meet up with regions which have been converted to true vacuum by other bubbles. Physically, τ represents the duration of the phase transition. Our results depend quantitatively upon the choice for the cutoff function, but the qualitative dependence is slight. Besides our standard gaussian function, Eq. (11), we have used the following different forms for the cutoff function $C(t)$:

$$C(t) = \begin{cases} 1, & 0 \le t \le \tau_c \\ \cos^2\left(\frac{\pi(t-\tau_c)}{2(\tau-\tau_c)}\right), & \tau_c \le t \le \tau; \end{cases} \tag{47a}$$

$$C(t) = \begin{cases} 1, & 0 \le t \le \tau_c \\ \frac{1}{4}\left(\frac{2t-\tau-\tau_c}{\tau-\tau_c}\right)^3 - \frac{3}{4}\left(\frac{2t-\tau-\tau_c}{\tau-\tau_c}\right) + \frac{1}{2}, & \tau_c \le t \le \tau. \end{cases} \tag{47b}$$

Moreover, we have varied the time τ_c at which the cutoff comes into play. The sensitivity of our numerical results to the choice of the cutoff are shown in Figs. 11 and 12.

(d) Summary of numerical results

To summarize, through numerical simulations we have established that the energy radiated in gravity waves in the collision of two vacuum bubbles depends upon only the grossest features of the bubble collision: the false-vacuum energy density $\rho_{\rm vac}$ and the duration of the collision (cutoff time τ), provided that the separation of the bubble centers d is comparable to τ and d is much greater than the initial size of the bubbles, R_0 (both assumptions are true in the cases of interest). In particular,

$$\frac{dE_{\rm GW}}{d\omega} \propto \rho_{\rm vac}^2 \tau^6; \qquad \omega_{\rm max}\tau \simeq 3.8;$$

$$\tilde{E}_{\rm GW} \simeq a\tilde{\rho}_{\rm vac}^2\tilde{\tau}^5; \tag{48}$$

where in the final expression $a \simeq 0.042$.

With this result in hand we compute the fraction of the total vacuum energy released that goes into gravitational waves. Neglecting the interaction of the two bubbles, at time τ the volume occupied by two bubbles separated by distance d is $4\pi\tau^3 g(\alpha)/3$, where the geometrical factor $g(\alpha) = 1 + 3/4\alpha - 1/16\alpha^3$ accounts for bubble overlap; the vacuum energy liberated is just this volume times $\rho_{\rm vac}$. For simplicity, we ignore the geometrical correction factor of order unity and write $E_{\rm vac} = 4\pi\tau^3\rho_{\rm vac}/3$; it then follows that the fraction of the vacuum energy released that goes into gravitational waves is given by

$$f \equiv \frac{E_{\rm GW}}{E_{\rm vac}} = \frac{3a\rho_{\rm vac}\tau^2}{4\pi}\left(\frac{\varphi_0}{m_{\rm Pl}}\right)^2, \tag{49}$$

which by relating $\rho_{\rm vac}$ to the Hubble parameter, $H^2 = 8\pi\rho_{\rm vac}/3{m_{\rm Pl}}^2$, can be written as

$$f = \frac{9a}{32\pi^2}\left(\frac{\tau}{H^{-1}}\right)^2 \simeq 1.3\times 10^{-3}\left(\frac{\tau}{H^{-1}}\right)^2. \tag{50}$$

That is, the efficiency of gravitational radiation depends upon the ratio of τ to the Hubble time; this is the result predicted in Ref. [10]. That this is the case is not completely surprising; recall that the Newtonian gravitational potential outside a bubble is $\phi/c^2 \sim (R/H^{-1})^2$, where $R \sim \tau$ is the size of the bubble; this implies that as $R/H^{-1} \to 1$ the gravitational field becomes strong. Also note that as $\tau \to H^{-1}$ our calculation becomes suspect, as we have linearized gravity, neglected the expansion of the Universe, and ignored gravitational effects in the bubble nucleation process. As we shall discuss in the next Section, in typical cosmological circumstances one expects τ/H^{-1} to be of the order of a few per cent.

(e) Unequal bubbles

Because of the massive computational resources required, our results for the unequal-bubble case are very limited. We have considered two cases. As viewed in the equal-bubble frame $d = 60$; the equal-bubble frame is related to the lab frame by a Lorentz boost along the z-axis of: (i) $\beta = 0.1$, corresponding to a difference of nucleation times of $\Delta t \simeq 6$ and a ratio of bubble radii when the bubbles first touch of about 1.22; (ii) $\beta = 0.2$, corresponding to a nucleation time difference of 12 and ratio of bubble radii at first touch of 1.5. Note the separation of the bubbles in the lab frame is $\sqrt{1-\beta^2}\,d \simeq 60$. Fig. 13 shows the energy spectrum of gravitational waves for these two cases, along with the equal-bubble case for comparison. For the unequal-bubble collisions the total energy radiated is smaller and the peak of the spectrum is shifted (slightly) to higher frequencies. This is consistent with our expectation that in an unequal-bubble collision it is the size of the smaller bubble that sets the length/time scale for the problem.

VI. Discussion and Concluding Remarks

(a) Bubble nucleation: expectations for τ and d

Our results depend sensitively upon the duration of the phase transition τ and rely upon the assumption that the bubble separation d is of the same order as the duration of the phase transition τ. To address both questions we briefly discuss bubble nucleation in a first-order phase transition. The bubble nucleation rate (per volume per time) is generally of the form $\Gamma = \mathcal{M}^4 \exp[-A(t)]$; the tunneling action A varies with time through its dependence upon the temperature (or the evolution of other fields) and, given a specific model, is straightforward to compute [12]. The prefactor is more difficult to compute and less important (all the "action" is the action); $\mathcal{M}$ is an energy scale characteristic of the phase transition, expected to be of the order of the fourth-root of the false-vacuum energy density (or equivalently, the phase-transition temperature). The completion of the phase transition occurs roughly when $\Gamma \sim H^4$, which corresponds to a nucleation rate of the order of one bubble per Hubble time per Hubble volume. Given $A(t)$, it is easy to describe the phase transition in detail: duration, distribution of bubble sizes, etc., and this is done in Ref. [21]. We quickly review the salient facts here.

First, expand the action around $t = t_*$, the time at which the phase transition completes:

$$A(t) = A_* + \dot{A}_*(t - t_*) + \cdots; \tag{51}$$

note that $\dot{A}_* \equiv [dA/dt]|_{t=t_*} < 0$. This expansion is general enough to describe most first-order phase transitions; moreover, it is the rate of change of the action that determines all quantities of interest here. Let H_* be the value of the Hubble constant at time t_*; we can solve for A_* by equating $\Gamma(t_*)$ to $H_*^4 \sim \mathcal{M}^8/m_{\rm Pl}{}^4$:

$$A_* \simeq 4\ln(m_{\rm Pl}/\mathcal{M}); \tag{52}$$

For simplicity, assume that bubbles are nucleated with zero initial size and expand at the speed of light. Then if $a(t)$ is the cosmological scale factor, the volume at time t of a bubble nucleated at time t' is

$$V(t,t') = \frac{4\pi}{3}\left[a(t)\int_{t'}^{t}\frac{du}{a(u)}\right]^3. \tag{53}$$

The probability that a point in space still remains in the false vacuum at time t is $p(t) = e^{-I(t)}$, where

$$I(t) = \int_0^t \Gamma(t')V(t,t')dt'. \tag{54}$$

The kinematics of bubble nucleation depends upon $\Gamma(t)$ and $I(t)$. At the end of the phase transition, the distribution of bubble sizes r is

$$\frac{dn}{dr} = \left\{a(t)^3\Gamma(t)e^{-I(t)}\right\}\Big|_{t=t(r)}; \tag{55}$$

where $t(r)$ is the time at which a bubble of size r was nucleated, defined implicitly by the equation $r = a(t)\int_{t(r)}^{t_*} du/a(u)$. We define the end of the phase transition ($t = t_*$) to be the time when the probability that a point in space remains in the false vacuum is very small, $p(t_*) = e^{-M}$, where $M \sim 10 - 30$ (*i.e.*, $I_* = M$) and the duration τ to be the time it takes $I(t)$ to increase from m to M, where $m \sim 0.1 - 1$. Matters simplify if we assume that the transition lasts a Hubble or less (corresponding to $|\dot{A}_*| \gtrsim H$); for most cases of interest, this is a good approximation. Making this assumption, the duration of the transition $\tau \simeq \ln(M/m)/|\dot{A}_*| \simeq few/|\dot{A}_*|$ and the distribution of bubble sizes

$$\frac{dn}{dr} = \frac{|\dot{A}_*|^4}{8\pi e} \exp[-(r - r_0)^2/2\sigma^2], \tag{56}$$

where $r_0 = \ln M/|\dot{A}_*|$ is the mean bubble size, $\sigma = 1/|\dot{A}_*| \simeq r_0/2$ is the gaussian width of the distribution, and the average distance between bubbles

$$d \equiv \left[\int_0^\infty \frac{dn}{dr} dr\right]^{-1/3} = \frac{2^{5/6}\pi^{1/6}e^{1/3}}{|\dot{A}_*|}. \tag{57}$$

Since our results depend only logarithmically upon the somewhat arbitrarily defined quantities M and m, we need not be too concerned with refining their definitions.

Based upon this simple model we see that duration of the phase transition, the typical bubble size, and the bubble separation are all comparable and determined by $|\dot{A}_*|$: in particular, $\tau \simeq few/|\dot{A}_*|$. Finally, let us relate $|\dot{A}_*|$ to A_*, and thereby to $\mathcal{M}$ or T_*. The tunneling action varies with time because of its temperature dependence (or the evolution of other fields); unless one "tunes" the parameters of the model, one would expect the timescale for change in the action to be comparable to the timescale on which the temperature changes, which implies that $dA/dt \sim A_*/H_*^{-1}$. If we define $|\dot{A}_*| = \beta A_* H$, we expect the dimensionless constant β to be of the order of unity. We can then write $\tau/H_*^{-1} \simeq few/\beta A_* \simeq 1/\ln(m_{\rm Pl}/\mathcal{M}) \sim 1/\ln(m_{\rm Pl}/T_*)$. For the temperatures of interest, say 1 GeV to 10^{15} GeV, τ/H_*^{-1} is expected to be order a few percent; thus $(\tau/H_*^{-1})^2 \sim 10^{-3}$, which implies that the fraction of vacuum energy converted into gravitational waves is of the order of 10^{-6} to 10^{-5}. (We note that in inflationary models associated with a first-order phase transition, referred to as extended or first-order inflation [9], τ/H_*^{-1} is usually close to unity [21], which is even more favorable for gravity-wave production.)

(b) Summary

We have numerically studied the collision of two bubbles of true vacuum in Minkowski space, and in the linearized-gravity approximation we have computed the amount of gravitational radiation produced in a time τ comparable to the bubble separation d. As we have discussed, both the linearized-gravity approximation and the neglect of the expansion of the Universe are good approximations for $\tau \lesssim H^{-1}$; further, in a realistic phase transition, one expects τ to be of the order of d. Most of the gravitational radiation

produced is associated with the bulk motion of the bubble walls and not the fine-scale oscillations associated with internal motions of the scalar field. Because of this fact, the gravitational radiation that arises from the collision of two vacuum bubbles is very simple to characterize. It depends only upon the duration of the phase transition τ and the false-vacuum energy density $\rho_{\rm vac}$. In particular, the spectrum $dE_{\rm GW}/d\omega \propto \rho_{\rm vac}^2 \tau^6$ and peaks at a characteristic frequency $\omega_{\rm max} \simeq 3.8/\tau$ (characteristic of the bubble wall curvature and not the thickness of the bubble wall). The fraction of the total vacuum energy liberated by the collision of two vacuum bubbles that is released in gravitational radiation is about $1.3 \times 10^{-3}(\tau/H^{-1})^2$.

While our results are based upon the full, linearized-gravity approximation (*i.e.*, sum of all multipoles), we also computed the gravitational radiation in the familiar "quadrupole approximation." Surprisingly we find that the quadrupole approximation *overestimates* the amount of gravitational radiation produced by a large factor (more than 50); since the full, linearized-gravity result is just the *incoherent* sum of *all* the multipoles, this presents a paradox. The resolution of this paradox is simple: The familiar "quadrupole approximation" (like its dipole counterpart in electromagnetism) involves an additional assumption: namely that the source size is small compared to the wavelength of the radiation produced, and this assumption is not satisfied in the present circumstance. The "true quadrupole" contribution to the full, linearized-gravity approximation is indeed smaller the sum of all the multipoles. Further, a simple analytic model described in Appendix B explains quite well the discrepancy between the full, linearized calculation and the familiar "quadrupole approximation."

The collision of two vacuum bubbles is a potent source of gravitational radiation; we expect that a fraction of order 10^{-6} or so of the vacuum energy released when vacuum bubbles collide goes into gravity waves. Careful estimates of the contribution of a strongly first-order phase transition to the stochastic background of gravitational radiation based upon the present work are made elsewhere [11].

It is a pleasure to acknowledge many stimulating conversations with Lawrence Widrow, and helpful conversations with E.W. Kolb, R.V. Wagoner, and R.M. Wald. This work was supported in part by the NSF (AK's graduate fellowship), by the DOE (at Chicago and Fermilab), and by the NASA through grant NAGW 2381 (at Fermilab).

Note added: After this work was completed we became aware of a similar numerical study by M. Shibata and Y. Nambu (Kyoto University preprint 1095). Their results for the amount of gravitational radiation produced by bubble collisions are significantly smaller than ours (some 6 orders of magnitude) and the conclusions they draw very different.

Appendix A: Stress-tensor Components

This Appendix contains the complete formulas for the relevant components of the Fourier-transformed stress tensor in the case of two vacuum bubbles nucleated simultaneously. The subscripts "1" and "2" refer to two different regions of integration prior to the hyperbolic change of variables, Eqs. (26), and $r^2 = x^2 + y^2$. A given component of the stress tensor is a sum of the "1" and "2" contributions. The T^{xy} and T^{yz} components are zero since we have taken $\mathbf{k}_y = 0$.

For $r^2 < t^2$ (region 1):

$$T_1^{xx}(\hat{\mathbf{k}},\omega) = \frac{1}{2}\int_0^\infty s^2\,ds \int_{-\infty}^\infty dz\, e^{i\omega_z z}\Big(\frac{\partial\varphi}{\partial s}\Big)^2 \int_1^\infty du(u^2-1)e^{i\omega su} \times [J_0(\omega_x s\sqrt{u^2-1}) - J_2(\omega_x s\sqrt{u^2-1})]\,C(su) \quad (A1)$$

$$T_1^{yy}(\hat{\mathbf{k}},\omega) = \frac{1}{2}\int_0^\infty s^2\,ds \int_{-\infty}^\infty dz\, e^{i\omega_z z}\Big(\frac{\partial\varphi}{\partial s}\Big)^2 \int_1^\infty du(u^2-1)e^{i\omega su} \times [J_0(\omega_x s\sqrt{u^2-1}) + J_2(\omega_x s\sqrt{u^2-1})]\,C(su) \quad (A2)$$

$$T_1^{zz}(\hat{\mathbf{k}},\omega) = \int_0^\infty s^2\,ds \int_{-\infty}^\infty dz\, e^{i\omega_z z}\Big(\frac{\partial\varphi}{\partial z}\Big)^2 \int_1^\infty du\, e^{i\omega su} J_0(\omega_x s\sqrt{u^2-1})\,C(su) \quad (A3)$$

$$T_1^{xz}(\hat{\mathbf{k}},\omega) = -i\int_0^\infty s^2\,ds \int_{-\infty}^\infty dz\, e^{i\omega_z z}\Big(\frac{\partial\varphi}{\partial s}\Big)\Big(\frac{\partial\varphi}{\partial z}\Big) \int_1^\infty du\sqrt{u^2-1}e^{i\omega su} \times J_1(\omega_x s\sqrt{u^2-1})\,C(su) \quad (A4)$$

For $r^2 > t^2$ (region 2):

$$T_2^{xx}(\hat{\mathbf{k}},\omega) = \frac{1}{2}\int_0^\infty s^2\,ds \int_{-\infty}^\infty dz\, e^{i\omega_z z}\Big(\frac{\partial\varphi}{\partial s}\Big)^2 \int_0^\infty du(u^2+1)e^{i\omega su} \times [J_0(\omega_x s\sqrt{u^2+1}) - J_2(\omega_x s\sqrt{u^2+1})]\,C(su) \quad (A5)$$

$$T_2^{yy}(\hat{\mathbf{k}},\omega) = \frac{1}{2}\int_0^\infty s^2\,ds \int_{-\infty}^\infty dz\, e^{i\omega_z z}\Big(\frac{\partial\varphi}{\partial s}\Big)^2 \int_0^\infty du(u^2+1)e^{i\omega su} \times [J_0(\omega_x s\sqrt{u^2+1}) + J_2(\omega_x s\sqrt{u^2+1})]\,C(su) \quad (A6)$$

$$T_2^{zz}(\hat{\mathbf{k}},\omega) = \int_0^\infty s^2\,ds \int_{-\infty}^\infty dz\, e^{i\omega_z z}\Big(\frac{\partial\varphi}{\partial z}\Big)^2 \int_0^\infty du\, e^{i\omega su} J_0(\omega_x s\sqrt{u^2+1})\,C(su) \quad (A7)$$

$$T_2^{xz}(\hat{\mathbf{k}},\omega) = i\int_0^\infty s^2\,ds \int_{-\infty}^\infty dz\, e^{i\omega_z z}\Big(\frac{\partial\varphi}{\partial s}\Big)\Big(\frac{\partial\varphi}{\partial z}\Big) \int_0^\infty du\sqrt{u^2+1}e^{i\omega su} \times J_1(\omega_x s\sqrt{u^2+1})\,C(su) \quad (A8)$$

where $\hat{\mathbf{k}}_z = \cos\theta$, $\omega_z = \omega\cos\theta$, $\omega_x = \omega\sin\theta$; J_n is the Bessel function of order n; and $C(x)$ is the cutoff function, cf., Eqs. (11, 47ab). As discussed in Section II, the scalar field φ is a function only of s and z.

Appendix B: Resolution of a Paradox

It may seem paradoxical that the flux of gravitational waves is *smaller* when calculated in the full-linearized approximation (linear gravity, fully relativistic treatment) than in the quadrupole approximation (linearized gravity, lowest-order in v/c). After all, shouldn't the total energy radiated be given by an *incoherent* sum of all multipoles—quadrupole, octupole, and so? The answer is yes and no! We will elucidate this interesting and important point by first examining the electromagnetic analogue.

(a) Multipole electromagnetic radiation

Linearized gravity is like electromagnetic theory with an extra index. Thus the treatment of electromagnetic multipole radiation provides a simple and familiar example to illustrate the underlying reason why the radiation in the "full" calculation can indeed be less than that given by the quadrupole formula.

Recall the multipole formalism of electromagnetic radiation [22]. In the far-zone (distance $r \gg$ wavelength $\lambda = 2\pi/k$), $\mathbf{E}$ and $\mathbf{B}$ are expanded in vector-spherical harmonics, $\mathbf{X}_{lm}$ and $\mathbf{n}\times\mathbf{X}_{lm}$ ($l = 1, 2, 3, \cdots$; $m = -l, -l+1, \cdots l-1, l$):

$$\mathbf{B} \to \frac{e^{i\mathbf{k}\cdot\mathbf{r}-i\omega t}}{kr}\sum_{l,m}(-i)^{l+1}\left[a_E(l,m)\mathbf{X}_{lm} + a_M(l,m)\mathbf{n}\times\mathbf{X}_{lm}\right], \qquad (B1a)$$

$$\mathbf{E} \to \mathbf{B}\times\mathbf{n}, \qquad (B1b)$$

where $|\mathbf{k}| = \omega$, $\mathbf{n}$ is the unit vector in the radial direction, and for simplicity, just a single mode is considered (which is easily generalized to a Fourier integral). The power radiated in electromagnetic waves is given by the incoherent sum over multipoles:

$$P = \frac{1}{8\pi k^2}\sum_{l,m}\left[|a_E(l,m)|^2 + |a_M(l,m)|^2\right]. \qquad (B2)$$

The electric- and magnetic-multipole amplitudes are obtained by solving the field equations in the near zone and matching to the far-zone solutions, Eq. (B1). In particular, the electric-multipole amplitudes $a_E(l,m)$ and magnetic-multipole amplitudes $a_M(l,m)$ can be expressed in terms of integrals over the source:

$$a_E(l,m) = -i\frac{4\pi k^2}{\sqrt{l(l+1)}}\int Y^*_{lm}\left\{\rho\frac{\partial}{\partial r}\left[rj_l(kr)\right] + ik(\mathbf{r}\cdot\mathbf{J})j_l(kr)\right\}d^3x, \qquad (B3a)$$

$$a_M(l,m) = -i\frac{4\pi k^2}{\sqrt{l(l+1)}}\int Y^*_{lm}\left\{\nabla\cdot(\mathbf{r}\times\mathbf{J})j_l(kr)\right\}d^3x; \qquad (B3b)$$

where $j_l(kr)$ is the spherical-Bessel function of order l, $\rho(\mathbf{x})e^{-i\omega t}$ is the charge density, $\mathbf{J}(\mathbf{x})e^{-i\omega t}$ is the current density, and for simplicity the magnetization term has been left out. These results are exact.

The lowest-order term, $a_E(1,m)$, is the electric-dipole term; as is clear from Eq. (B2), *the total power radiated must be greater than this term.* However, the form for $a_E(1,m)$ is *not* familiar. That is because an additional approximation is usually made when computing $a_E(1,m)$: the assumption that $kr_{\max} \ll 1$; *i.e.*, that the source dimensions ($\lesssim r_{\max}$) are small compared to the wavelength of the radiation. In this limit we can use the fact that $j_l(x) \to x^l/(2l+1)!!$ for $x \ll 1$ to write all the multipole amplitudes in more familiar forms:

$$a_E(l,m) = -i\frac{4\pi k^{l+2}}{(2l+1)!!}\sqrt{\frac{l+1}{l}}\int r^l Y^*_{lm}\rho d^3x, \qquad (B4a)$$

$$a_M(l,m) = -i\frac{4\pi k^{l+2}}{(2l+1)!!}\sqrt{\frac{1}{l(l+1)}}\int r^l Y^*_{lm}\nabla\cdot(\mathbf{r}\times\mathbf{J})d^3x. \qquad (B4b)$$

Now the electric dipole takes on its familiar form. In the limit of a small source, $kr_{\max} \ll 1$, the total power emitted must be greater than that given by the familiar dipole term. This is also true for a large source, $kr_{\max} \gtrsim 1$, provided that the exact expression, Eq. (B3a), is used for $a_E(1,m)$.. The dipole radiation given by the familiar small-source approximation can be larger than the exact expression for dipole radiation, and so the total power emitted need not be larger than that given by the "small-source" (*i.e.*, familiar) dipole expression. When the small-source approximation is used for a large source, one is assuming that the radiation from throughout the source adds coherently—a most "favorable" assumption.

(b) Multipole gravitational radiation

The multipole formalism and result generalizes readily to gravitational waves; we will present a brief sketch. To make the analogy as close as possible the equations in the gravitational-wave case will be denoted by primes on the equation numbers, corresponding to their electromagnetic analogues. For a more complete presentation of the multipole expansion of gravitational waves, see Ref. [9].

The transverse-traceless part of the metric perturbation, which describes the gravitational radiation, can be expanded in the far-zone region in tensor-spherical harmonics:

$$h^{TT}_{jk} = \frac{G}{r}\sum_{l=2}^{\infty}\sum_{m=-l}^{l}\left\{\frac{d^l}{dt^l}I^{lm}(t-r)T^{E2,lm}_{jk} + \frac{d^l}{dt^l}S^{lm}(t-r)T^{B2,lm}_{jk}\right\}, \qquad (B1')$$

where the I^{lm} are the "mass-multipole moments," the S^{lm} are the "current-multipole moments," and $T^{E2,lm}_{jk}$ and $T^{B2,lm}_{jk}$ are the "pure spin-2" tensor harmonics, which are linear combinations of the six, orthonormal tensor harmonics, $T^{\lambda l',lm}_{jk}$ ($\lambda = 0$ and $l' = l$; $\lambda = 2$ and $l' = l \pm 0, \pm 1, \pm 2$).

The power radiated in gravitational waves is given by the incoherent sum of the multipole moments:

$$P_{\rm GW} = \frac{G}{32\pi}\sum_{l,m}\left\{|d^{l+1}I^{lm}/dt^{l+1}|^2 + |d^{l+1}S^{lm}/dt^{l+1}|^2\right\}. \qquad (B2')$$

As in the electromagnetic case the multipole moments are obtained by matching the near-zone solution to the far-zone solution, Eq. (B1′), and can be written as integrals over the stress-energy tensor of the source:

$$\frac{d^l}{dt^l}I^{lm}(t) = (-i)^{l+2}8\int e^{-i\omega(t-t')}\left[\sqrt{\frac{(l+1)(l+2)}{2(2l-1)(2l+1)}}[T^{2l-2,lm}_{pq}(\Omega)]^* j_{l-2}(\omega r)\right.$$
$$\left.-\sqrt{\frac{3(l-1)(l+2)}{(2l-1)(2l+3)}}[T^{2l,lm}_{pq}(\Omega)]^* j_l(\omega r) + \sqrt{\frac{l(l-1)}{2(2l+1)(2l+3)}}[T^{2l+2,lm}_{pq}(\Omega)]^* j_{l+2}(\omega r)\right]$$
$$\times\tau_{pq}(t',r,\Omega)r^2 dr d\Omega dt' d\omega; \qquad (B3'a)$$

$$\frac{d^l}{dt^l}S^{lm}(t) = (-i)^{l+2}8\int e^{-i\omega(t-t')}\left[\sqrt{\frac{l+2}{2l+1}}[T^{2l-1,lm}_{pq}(\Omega)]^* j_{l-1}(\omega r)\right.$$
$$\left.-\sqrt{\frac{l-1}{2l+1}}[T^{2l+1,lm}_{pq}(\Omega)]^* j_{l+1}(\omega r)\right]\tau_{pq}(t',r,\Omega)r^2 dr d\Omega dt' d\omega; \qquad (B3'b)$$

where τ_{pq} is the sum of the stress-energy tensor of matter (T_{pq}) and the Landau-Lifshitz pseudotensor for the effective stress-energy of the gravitational field. In the present circumstance gravity is weak and we work only to linear order, thus $\tau_{pq} = T_{pq}$. The lowest-order term in the expansion is the mass quadrupole ($l = 2$); from Eq. ($B2'$) it is clear that the total power radiated must be greater than that given by the mass quadrupole, as the multipoles add incoherently to give the total power emitted.

The form of the quadrupole (and other multipoles) in Eq. ($B3'$a) is unfamiliar; if we take the small-source ($kr_{\rm max} \ll 1$), weak-field limit the familiar multipole formulas obtain:

$$I^{lm} = \frac{16\pi}{(2l+1)!!}\sqrt{\frac{(l+1)(l+2)}{2l(l-1)}}\int[Y^{lm}]^*\rho r^l d^3x; \qquad (B4'a)$$

$$S^{lm} = \frac{-32\pi}{(2l+1)!!}\sqrt{\frac{(l+2)(2l+1)}{2(l-1)(l+1)}}\int(\epsilon_{jpq}x_p\rho v_q)[Y^{l-1,lm}_j]^* r^{l-1}d^3x; \qquad (B4'b)$$

where the $Y^{l',lm}_j$ are a different representation of the vector-spherical harmonics. As in the electromagnetic analogue, it is not true that the small-source (*i.e.*, familiar) quadrupole approximation must give a result that is smaller than the sum of all multipoles.

(c) A simple model for colliding vacuum bubbles

By constructing a simple model for the collision of two vacuum bubbles we can also illustrate how it is that the flux of gravitational waves computed to all orders in the full-linearized theory ("full") is *less* than that computed in the familiar "quadrupole approximation" ("quad"). In the collision of two vacuum bubbles most of the "action" is along the z-axis (the axis joining the bubble centers); in the x-y plane the scalar field is relatively "quiet." Thus as a simple approximation we model the stress-energy tensor as

$$T^{ij}(\mathbf{x},t) = T^{ij}(z,t)\Theta(r)\Theta(L-r), \tag{B5}$$

where r is the radial coordinate in the x-y plane, $\Theta(r)$ is the Heaviside function, L is the characteristic radial size of the collision region, expected to be of order half the separation of the bubbles, *i.e.*, $L \sim d/2$.

From Eq. (B5) it follows that the desired Fourier transform of $T^{ij}(\mathbf{x},t)$ is given by

$$T^{ij}(\mathbf{k},\omega) = 2\pi L^2 T^{ij}(k_z,\omega)\frac{J_1(\omega L\sin\theta)}{\omega L\sin\theta}, \tag{B6}$$

where θ is the usual polar angle ($k_z = \omega\cos\theta$) and J_1 is the first-order Bessel function. Further, it then follows that

$$\frac{dE^{\rm full}}{d\Omega d\omega} = G\sin^4\theta\omega^2|t(k_z,\omega)|^2\left[\frac{2\pi L^2 J_1(\omega L\sin\theta)}{\omega L\sin\theta}\right]^2, \tag{B7a}$$

$$\frac{dE^{\rm quad}}{d\Omega d\omega} = G\sin^4\theta\omega^2|t(k_z=0,\omega)|^2\left[\pi L^2\right]^2, \tag{B7b}$$

where "full" and "quad" refer to the full, linearized-gravity calculation and the quadrupole approximation, and $t\hat{\mathbf{z}}\hat{\mathbf{z}}$ is the trace-free part of T^{ij} and $t = 2T^{zz}/3 - (T^{xx}+T^{yy})/3$. If we neglect the k_z dependence of $t(k_z,\omega)$, then it follows that

$$\frac{dE^{\rm full}/d\Omega d\omega}{dE^{\rm quad}/d\Omega d\omega} \approx \left[\frac{2J_1(\omega L\sin\theta)}{\omega L\sin\theta}\right]^2. \tag{B8}$$

Note that

$$\left[\frac{2J_1(\omega L\sin\theta)}{\omega L\sin\theta}\right]^2 \to \begin{cases} 1, & \omega L\sin\theta \ll 1; \\ 8\cos^2(\omega L\sin\theta - 3\pi/4)/\pi(\omega L\sin\theta)^3, & \omega L\sin\theta \gg 1. \end{cases}$$

This implies that the sum of all multipoles always gives a smaller result than the familiar "quadrupole approximation."

Finally, we can derive an approximate expression for $dE/d\omega$ based upon Eq. (B8):

$$\frac{dE^{\rm approx}}{d\omega} = 4\pi\frac{dE^{\rm quad}(\theta=\pi/2)}{d\Omega d\omega}\int_0^1\left[\frac{2J_1(\omega L\sin\theta)}{\omega L\sin\theta}\right]^2\sin^4\theta d\cos\theta, \tag{B9}$$

In Fig. 14, we show $dE/d\omega$ for $d = 240$ ($\alpha = 1.2$). The solid curve is our numerical calculation. The dotted curve is approximation (B9) derived from the numerically calculated quadrupole spectrum, using $L = \tau/2 = 1.2d/2$. The agreement is remarkably good for this very simple model.

References

[1] K.S. Thorne, in *300 Years of Gravitation*, edited by S. Hawking and W. Israel (Cambridge University Press, Cambridge, 1987) and references therein.

[2] See, *e.g.*, R. Vogt, "The U.S. LIGO Project" (Caltech preprint, 1991).

[3] V.A. Rubakov, M. Sazhin, and A. Veryaskin, *Phys. Lett. B* **115**, 189 (1982); R. Fabbri and M. Pollack, *ibid* **125**, 445 (1983).

[4] T. Vachaspati and A. Vilenkin, *Phys. Rev. D* **31**, 3052 (1985); T. Vachaspati, A.E. Everett, and A. Vilenkin, *ibid* **30**, 2046 (1984); B. Allen and E.P.S. Shellard, University of Wisconsin-Milwaukee preprint WISC-MILW-91-TH-12 (1991); R.R. Caldwell and B. Allen, University of Wisconsin-Milwaukee preprint WISC-MILW-91-TH-14 (1991) (submitted to *Phys. Rev. D*).

[5] M.S. Turner and N. Turok, work in preparation (1991).

[6] M. Gleiser, *Phys. Rev. Lett.* **63**, 1199 (1989).

[7] C.J. Hogan, *Mon. Not. R. Astr. Soc.* **218**, 629 (1986); E. Witten, *Phys. Rev. D* **30**, 272 (1984); L.M. Krauss, Yale University preprint YCTP-P33-91 (1991).

[8] D.R. Stinebring *et al.*, *Phys. Rev. Lett.* **65**, 285 (1990); M.M. Davis *et al.*, *Nature* **315**, 547 (1985).

[9] First-order, or extended, inflation is discussed by D. La and P.J. Steinhardt, *Phys. Rev. Lett.* **62**, 376 (1989); E.J. Weinberg, *Phys. Rev. D* **40**, 3950 (1989); and E.W. Kolb, *Physica Scripta* **T36**, 199 (1991).

[10] M.S. Turner and F. Wilczek, *Phys. Rev. Lett.* **65**, 3080 (1990).

[11] A. Kosowsky, M.S. Turner, and R. Watkins, Fermilab preprint FNAL/PUB-91/333-A (1991) (submitted to *Phys. Rev. Lett.*).

[12] S. Coleman, *Phys. Rev. D* **15**, 2929 (1977); C. Callan and S. Coleman, *ibid* **16**, 1762 (1977).

[13] S. Coleman and F. De Luccia, *Phys. Rev. D* **21**, 3305 (1980).

[14] S.W. Hawking, J.M. Stewart, and I.G. Moss, *Phys. Rev. D* **26**, 2681 (1982).

[15] W.Z. Chao, *Phys. Rev. D* **28**, 1898 (1983). We have some minor technical quibbles with Chao; he claims, incorrectly we believe, that even in the case where the nucleated bubbles have finite size and only a future history, the double-bubble solution is $O(2,1)$ invariant.

[16] R. Watkins and L.M. Widrow, Fermilab preprint FNAL/PUB-91/164-A (1991) (*Nucl. Phys. B*, in press (1992)). The use of $O(2,1)$ symmetry in evolving the scalar field associated two vacuum bubbles is discussed in detail.

[17] See e.g., C.W. Misner, K.S. Thorne, and J.A. Wheeler, *Gravitation* (Freeman, San Francisco, 1973), or K. Thorne, *Rev. Mod. Phys.* **52**, 299 (1980) and references therein.

[18] S. Weinberg, *Gravitation and Cosmology* (Wiley, New York, 1972), Ch. 10.

[19] Note this is just the opposite of what occurs for oscillating string loops; there the ratio of total energy radiated in the full, linearized-gravity approximation to that in the quadrupole approximation is between 50 and 100; cf., the factor γ in Vachaspati and Vilenkin, Ref. [4].

[20] This scaling is an estimate based upon a simple model where the gravitational radiation is assumed to arise only from the bubble walls (*i.e.*, neglecting the interaction region where the bubbles overlap). The collision removes a portion of each bubble surface, so that the boundary of the two bubbles is nonspherical. The quadrupole moment of the boundary of the two bubbles scales as $d\tau^4\rho_{\rm vac}$ and the triple-time derivative of the quadrupole moment scales as this divided by τ^3, from which it follows that the energy radiated $E_{\rm GW} \sim GQ_3^2\tau \sim \rho_{\rm vac}^2 d^2\tau^3 \propto \tau^3$.

[21] M.S. Turner, E.J. Weinberg, and L.M. Widrow, Fermilab preprint FNAL/PUB-91/334-A (1991) (submitted to *Phys. Rev. D*).

[22] J.D. Jackson, *Classical Electrodynamics* (J. Wiley & Sons, NY, 1988), Ch. 16.

Figure Captions

Figure 1: The scalar-field potential, Eq. (2), plotted in dimensionless units for ϵ=0.033, 0.05, 0.1, and 0.15. Note that ϵ determines the ratio of the vacuum energy to the barrier height, while λ and φ_0 set the overall energy and length scales.

Figure 2: The evolution of two identical vacuum bubbles. From left to right and top to bottom, $t = 36$, 60, 72, and 96.

Figure 3: The size of the bubbles at (a) nucleation and at the cutoff time τ for (b) $\alpha = 1$ and (c) $\alpha = 2$ (we have done calculations for $\alpha = 1.2, 2.0, 2.5, 3.5, 5.0, 8.0$). An "x" marks each bubble's center. In this schematic illustration we have ignored bubble interactions.

Figure 4a: Radiation patterns, $dE_{\rm GW}/d\omega d\Omega$, shown about the symmetry axis. The patterns are for frequencies $\omega\tau = 2.2$, 5.0, and 11, in order of descending amplitude. Along the axis joining the bubble centers the total radiation is identically zero (by symmetry). At higher frequencies, the patterns develop more lobes, illustrating that higher multipoles dominate.

Figure 4b: Radiation patterns for higher frequencies $\omega\tau = 22$, 29, and 36 (not to scale). The dominance of successively higher multipoles at higher frequencies is very apparent.

Figure 5: The total radiation pattern $dE/d\Omega = \int (dE/d\omega d\Omega) d\omega$. The dotted line shows an unnormalized quadrupole pattern for comparison. The importance of higher multipoles is apparent.

Figure 6: A comparison of the energy spectrum in the quadrupole and full-linearized approximations, for $d = 240$, $\alpha = 1.2$. Note the quadrupole spectrum is the *larger* one (see Appendix B). As they must, the two calculations agree in the limit $\omega \to 0$.

Figure 7: The energy spectra for various initial bubble separations. The top curve is for $d = 60$; the curve second from the top is for $d = 100$. The other virtually indistinguishable curves are for $d = 160$, 240, 300, 480.

Figure 8: The energy spectrum (per logarithmic frequency interval). At low frequencies the energy per octave increases as $(\omega\tau)^{2.8}$; at high frequencies it decreases as $(\omega\tau)^{-1.8}$.

Figure 9: The total energy radiated as a function of $\rho_{\rm vac}$ for $d = 240$, $\alpha = 1.2$. The squares are for the potential in Eq. (2), and the triangles for the modified potential, Eq. (51). The straight line indicates the anticipated $E_{\rm GW} \propto {\rho_{\rm vac}}^2$ scaling.

Figure 10: Total energy radiated as a function of cutoff time $\tau = (\alpha^2 d^2 - R_0^2)^{1/2} \approx \alpha d$. For $1.2d \lesssim \tau \lesssim 2.2d$ the energy radiated scales as τ^5; for large τ the energy radiated increases less rapidly than τ^5 (for $\tau/d \gg 1$ we expect $E_{\rm GW} \propto \tau^3$).

Figure 11: Energy spectra for different cutoffs, for $d = 60$, $\alpha = 1.2$. In order of decreasing amplitude, the curves are for τ_c/τ=0.95, 0.90, 0.80, and 0.70. Our results are at least qualitatively insensitive to τ_c/τ.

Figure 12: Energy spectra for different forms of the cutoff function, for $d = 60$, $\alpha = 1.2$. In order of decreasing amplitude, the curves are for cubic, cosine and gaussian cutoffs, cf., Eqs. (11, 47ab).

Figure 13: Unequal-bubble collisions for $d = 60$, $\alpha = 1.2$. For reference the solid curve shows the spectrum for the equal bubble case; the squares are for $\beta = 0.1$ (ratio of bubble sizes at collision = 1.22); and the triangles are for $\beta = 0.2$ (ratio of bubble sizes at collision = 1.5).

Figure 14: A comparison of our numerical results for $dE/d\omega$ (solid curve) and the approximation for $dE/d\omega$ (dashed curve) described in Appendix B, Eq. (B9). Results are for $d = 240$, $\alpha = 1.2$, and $L = \tau/2 = 0.6d$.

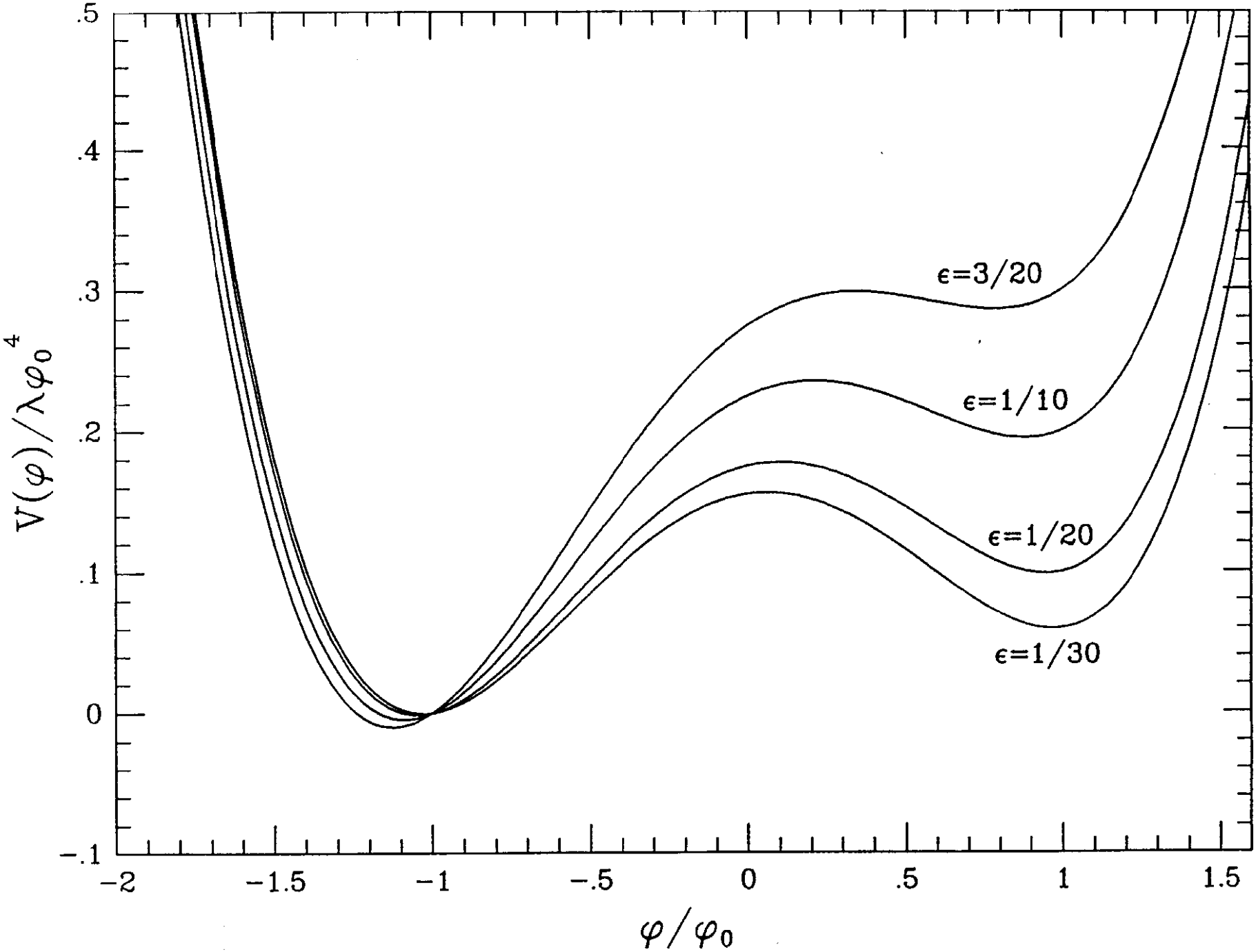
.5
.4
.3
.2
.1
0
−.1
−2
−1.5
−1
−.5
0
.5
1
1.5
$V(\varphi)/\lambda\varphi_0^4$
φ/φ_0
ϵ=3/20
ϵ=1/10
ϵ=1/20
ϵ=1/30

Figure 1

φ
z
r

φ
z
r

φ
z
r

φ
z
r

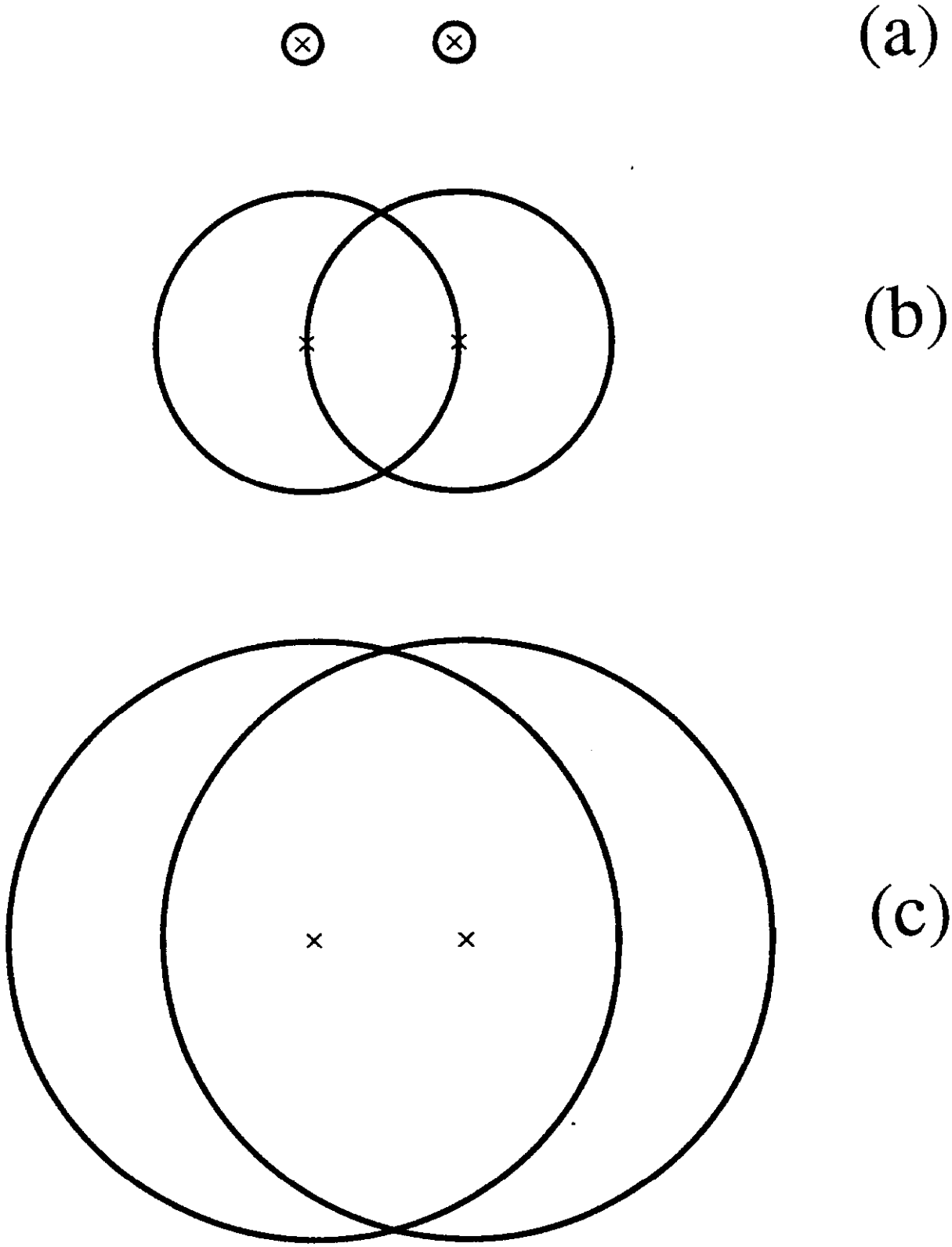

Figure 3

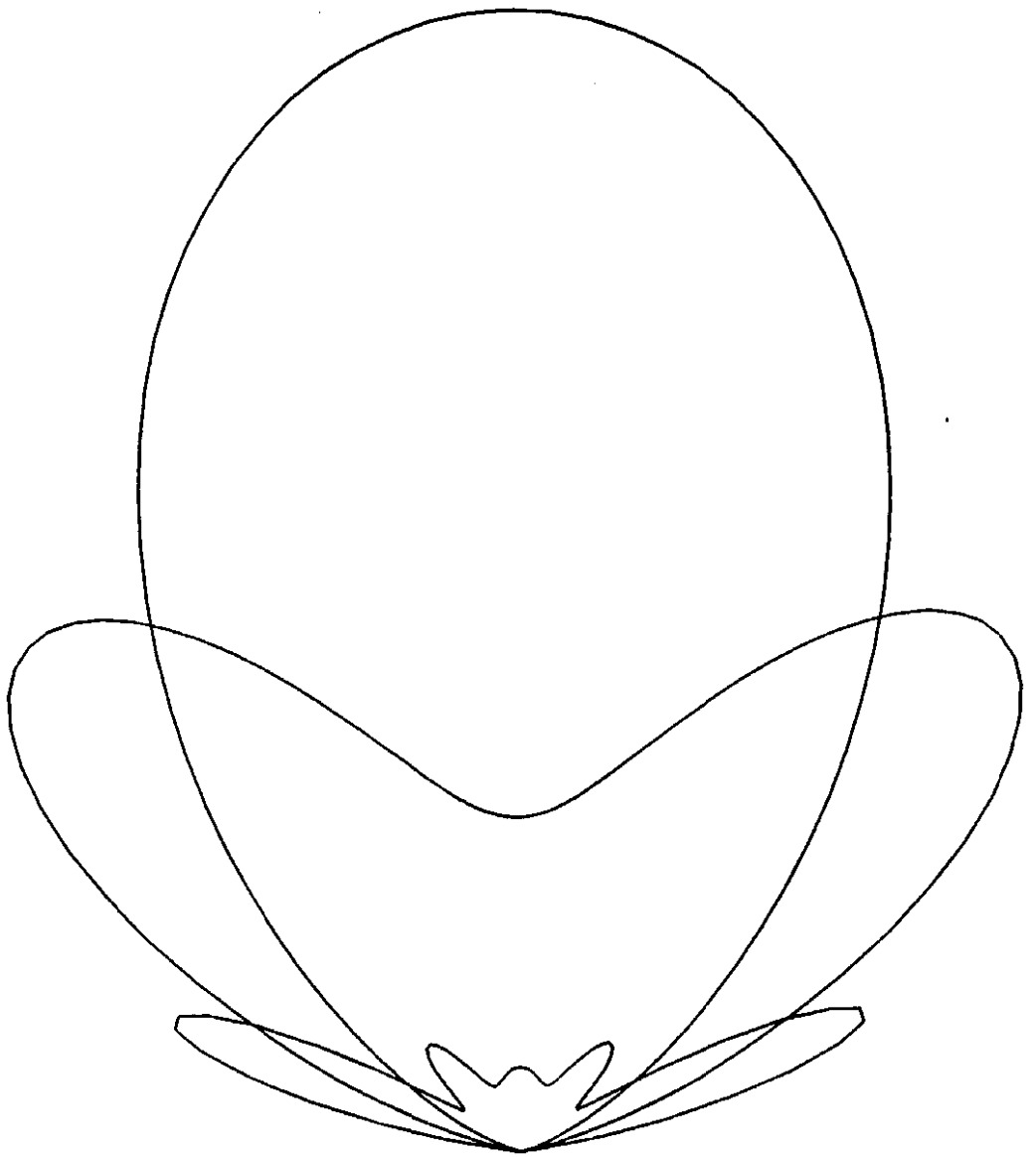

Figure 4a

$\omega\tau=22$

$\omega\tau=29$

$\omega\tau=36$

Figure 4b

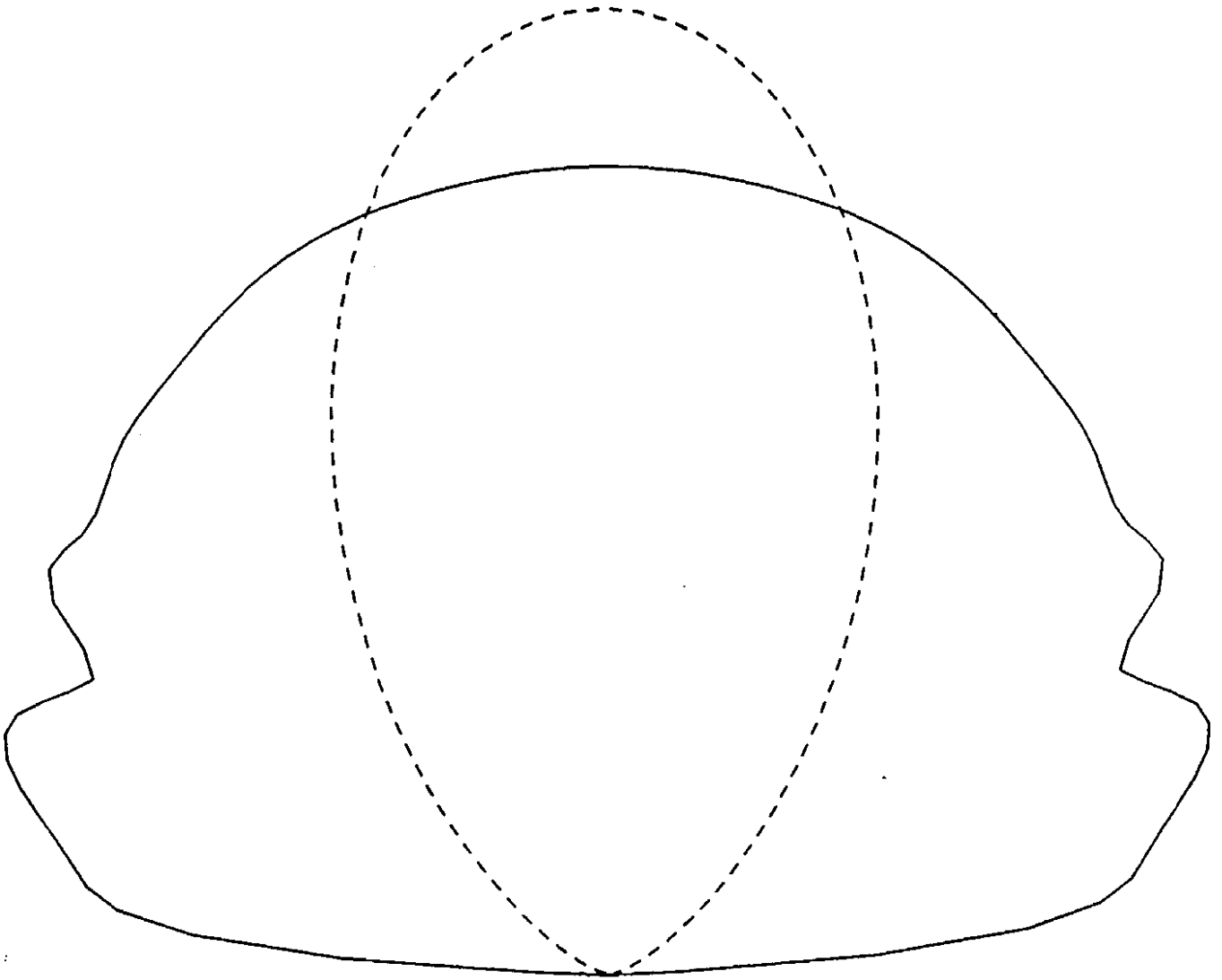

Figure 5

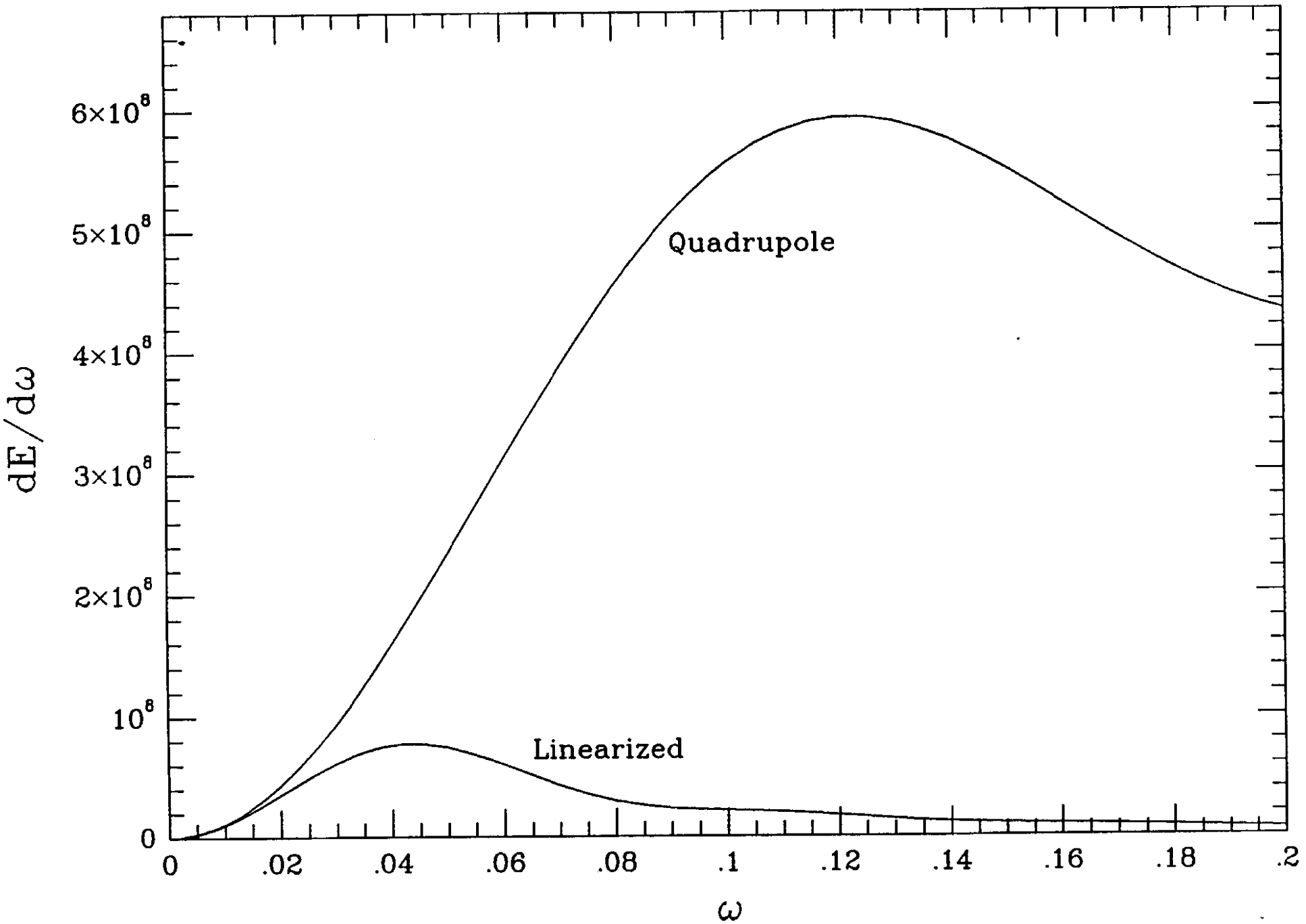
6×10^8
5×10^8
4×10^8
3×10^8
2×10^8
10^8
0
dE/dω
Quadrupole
Linearized
0
.02
.04
.06
.08
.1
.12
.14
.16
.18
.2
ω

Figure 6

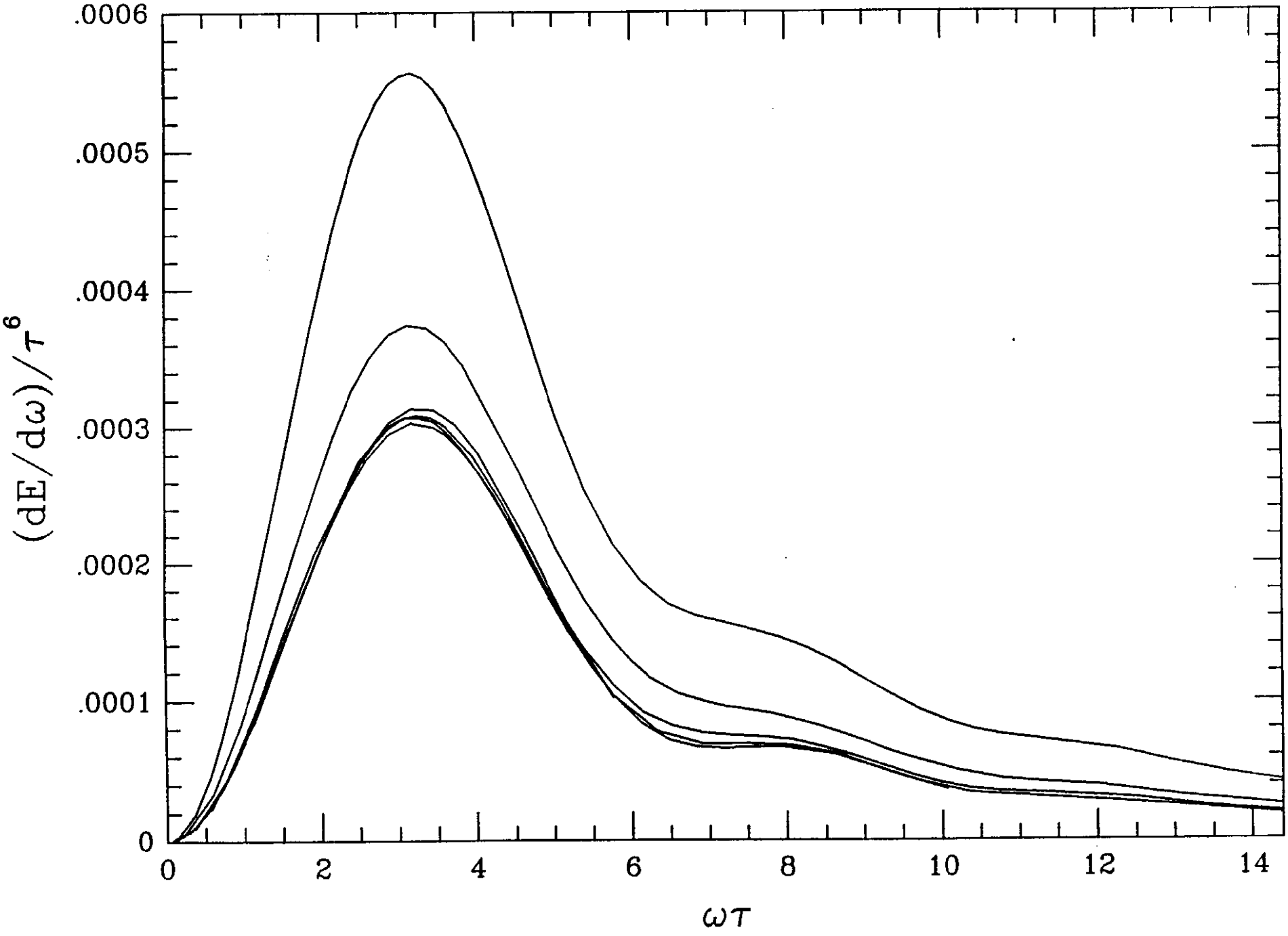
.0006
.0005
.0004
.0003
.0002
.0001
0
$(dE/d\omega)/\tau^6$
0
2
4
6
8
10
12
14
$\omega\tau$

Figure 7

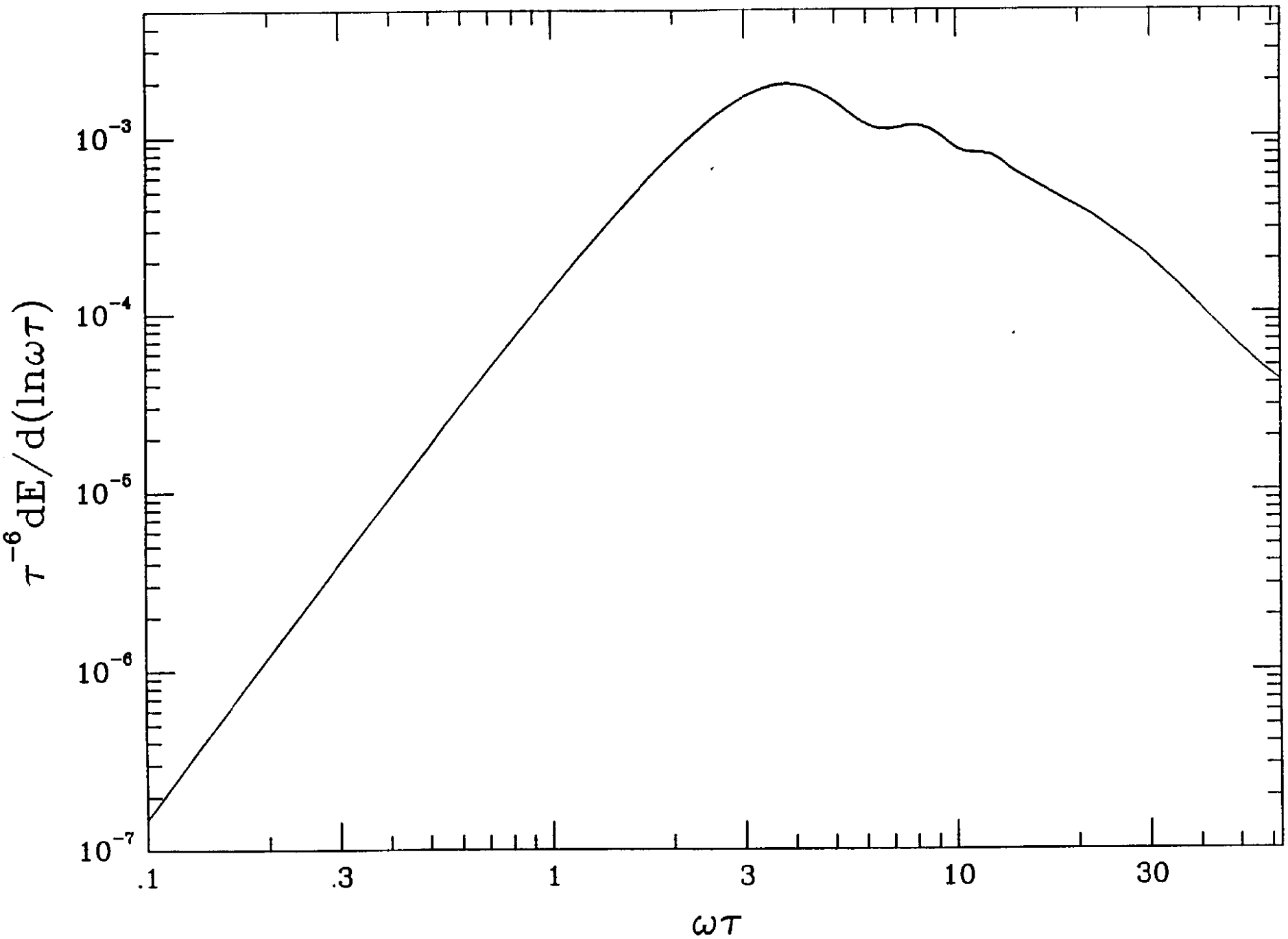

Figure 8

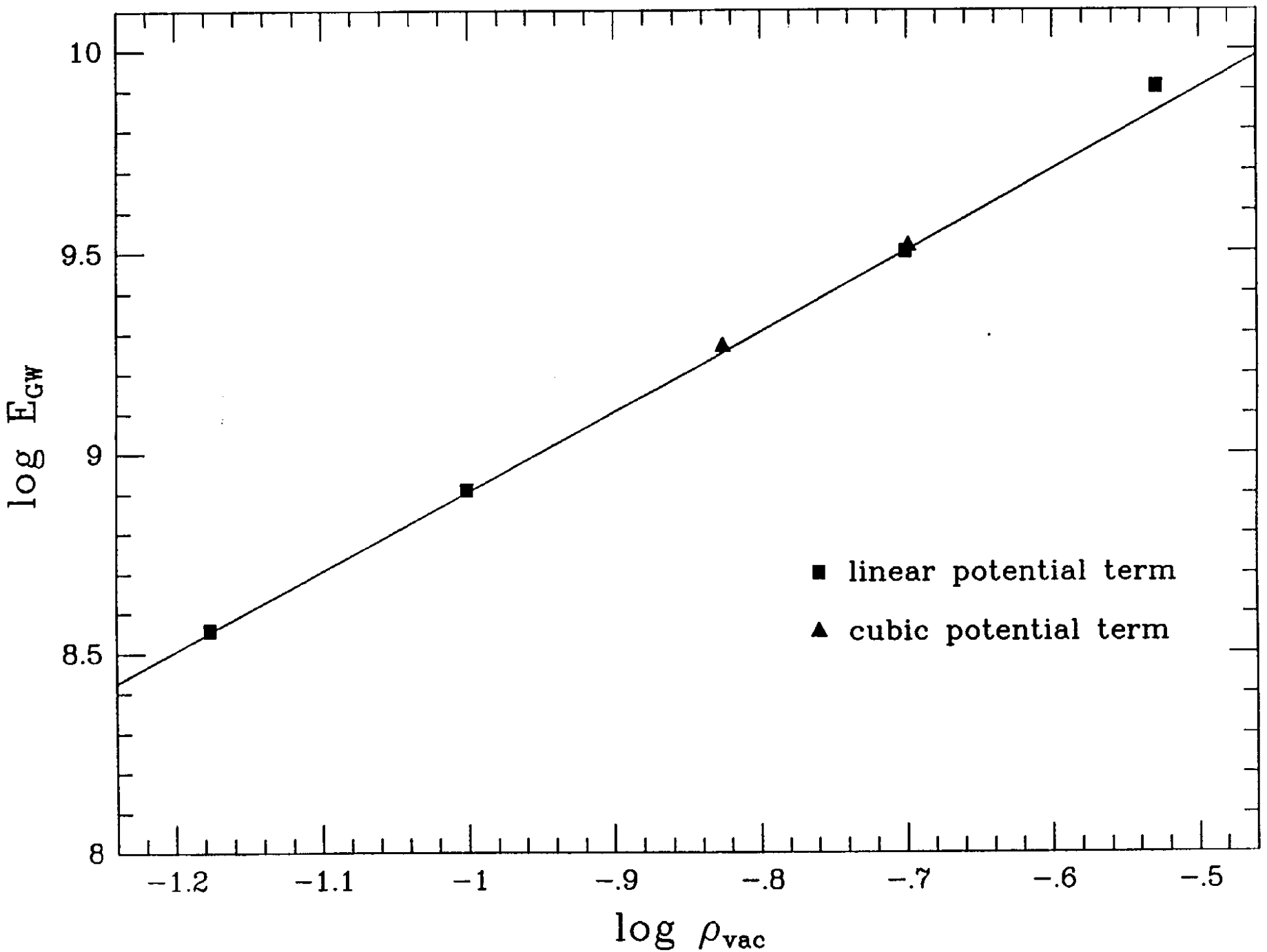
10
9.5
9
8.5
8
log E_{GW}
−1.2
−1.1
−1
−.9
−.8
−.7
−.6
−.5
log ρ_{vac}
linear potential term
cubic potential term

Figure 9

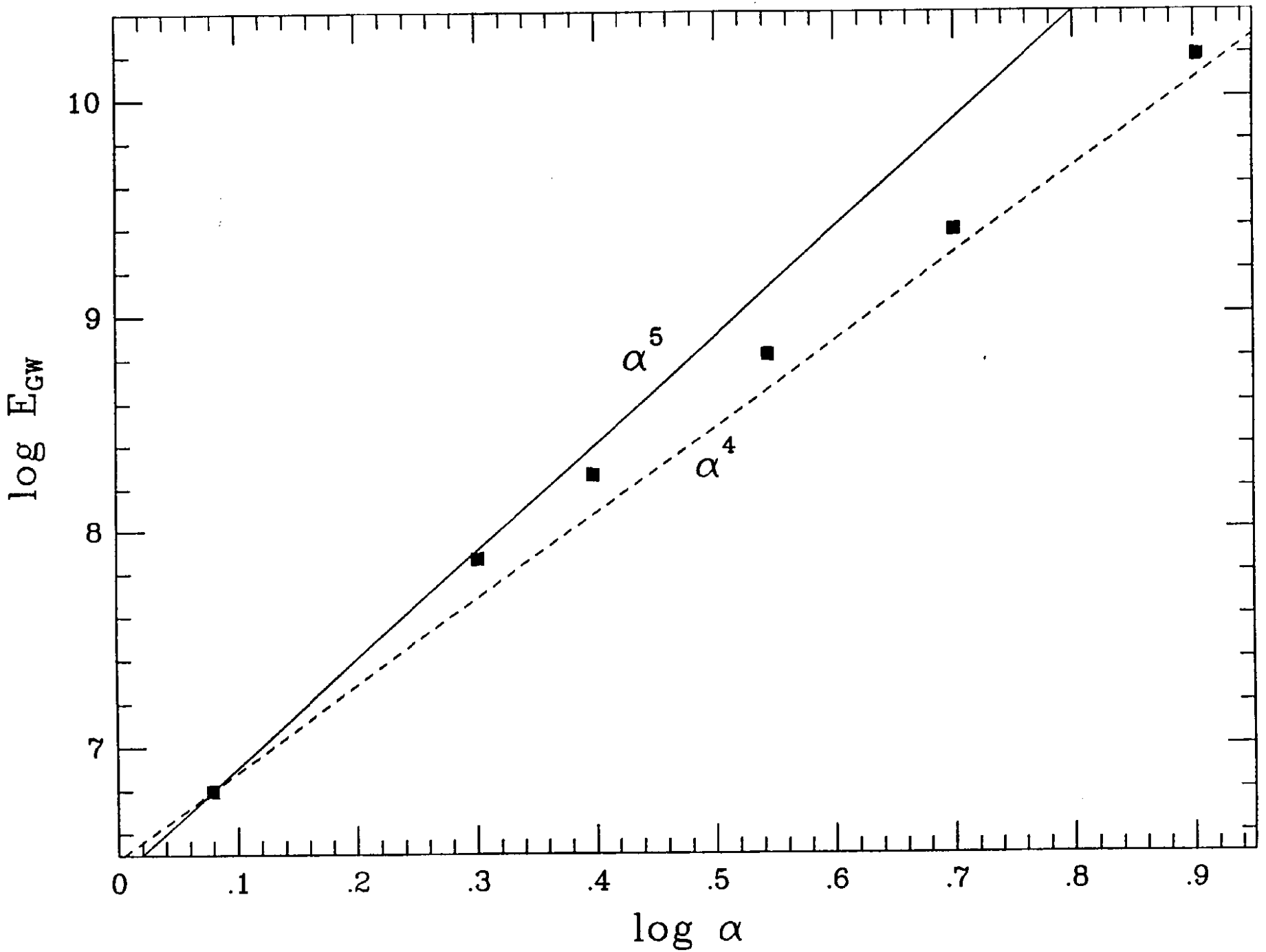

Figure 10

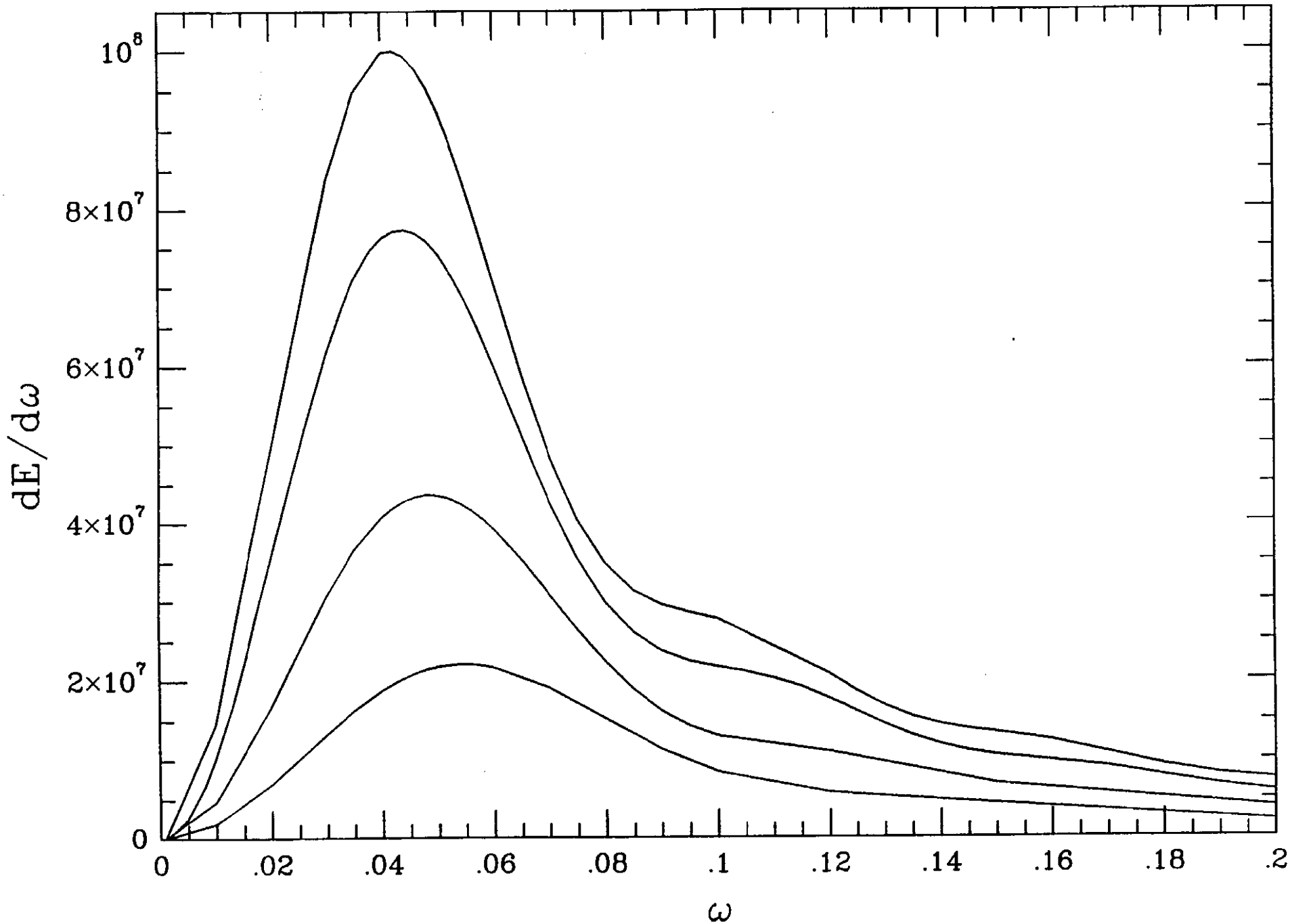
10^8
8×10^7
6×10^7
4×10^7
2×10^7
0
dE/dω
0
.02
.04
.06
.08
.1
.12
.14
.16
.18
.2
ω

Figure 11

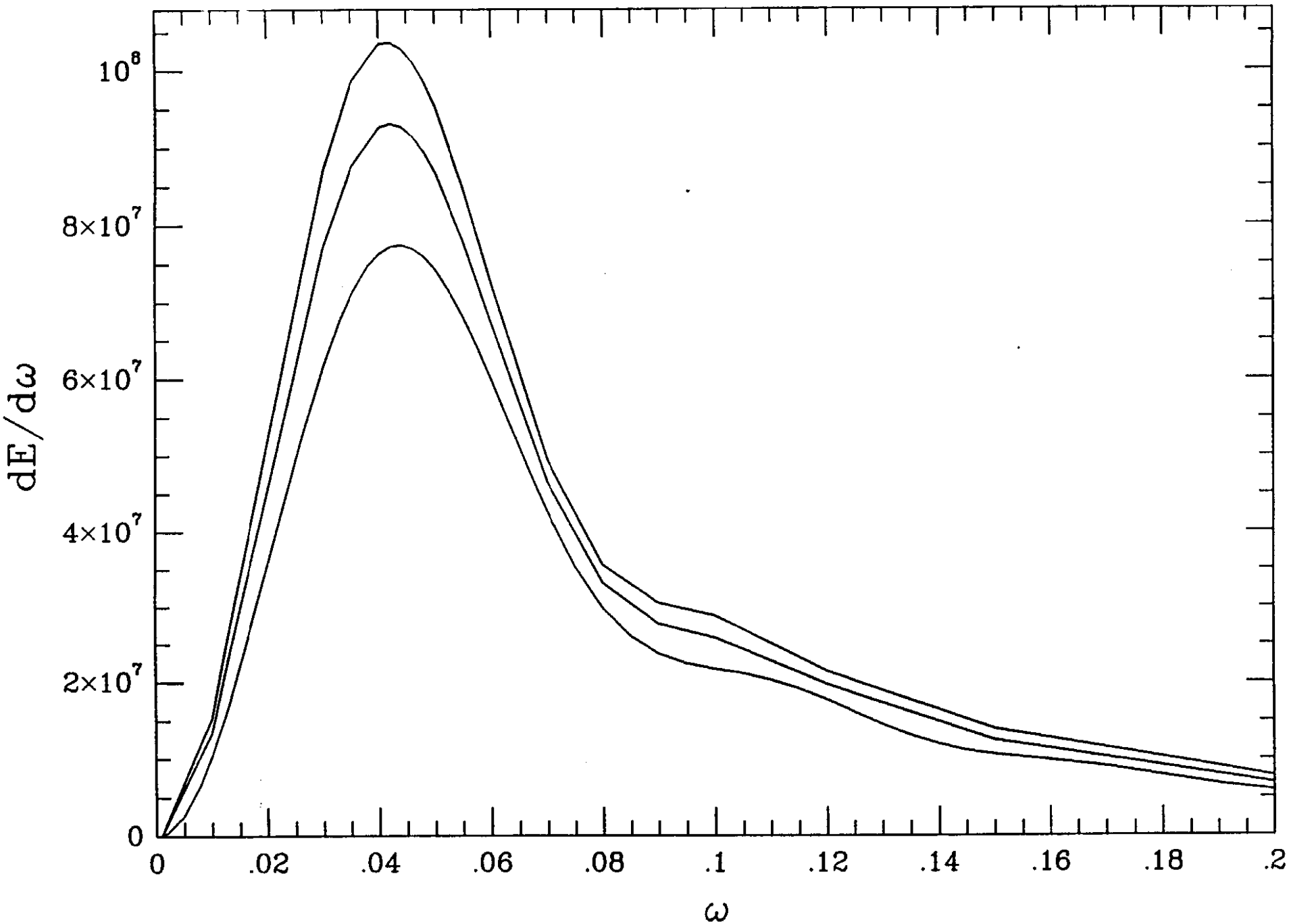
10^8
8×10^7
6×10^7
4×10^7
2×10^7
0
dE/dω
0
.02
.04
.06
.08
.1
.12
.14
.16
.18
.2
ω

Figure 12

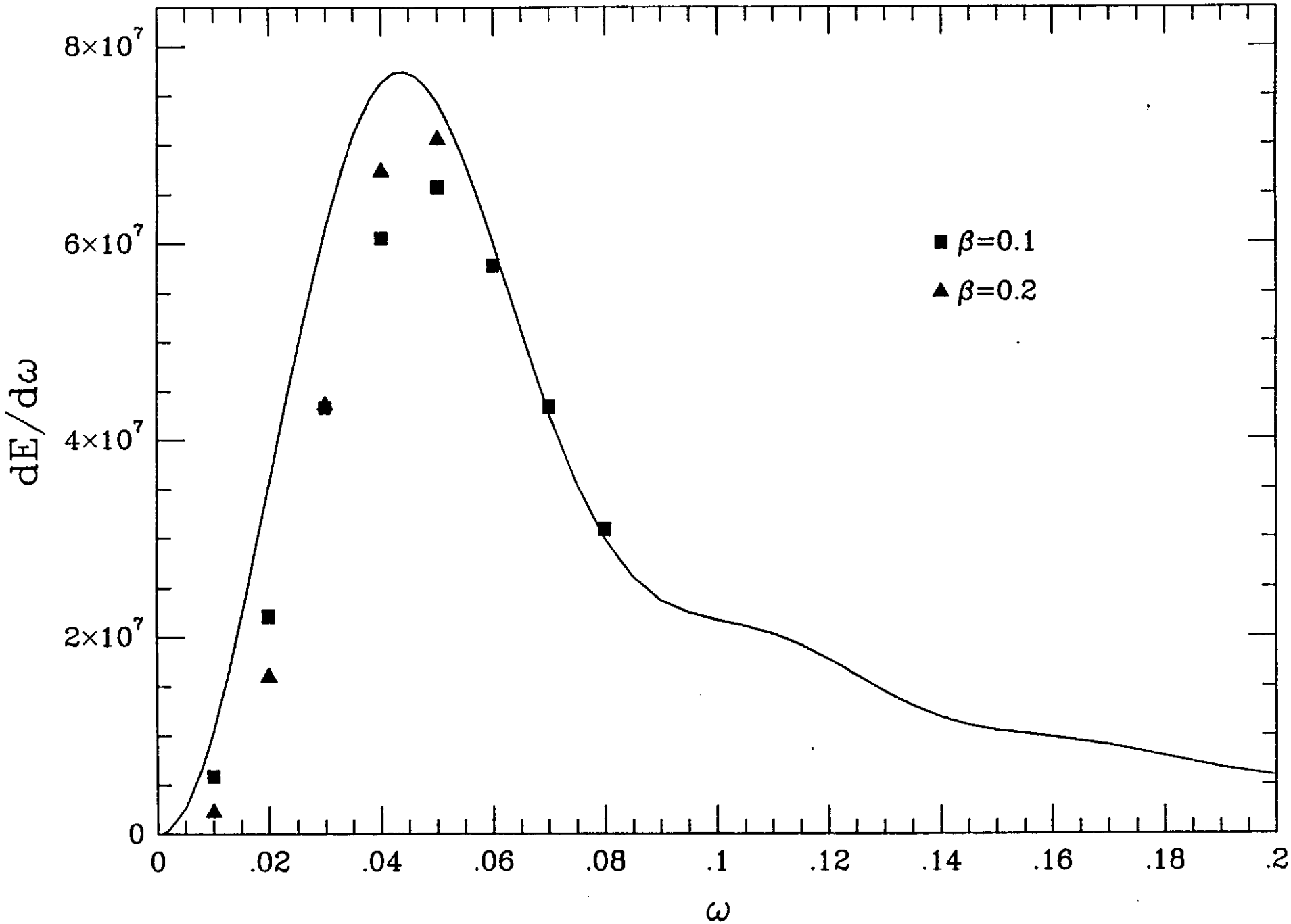

Figure 13

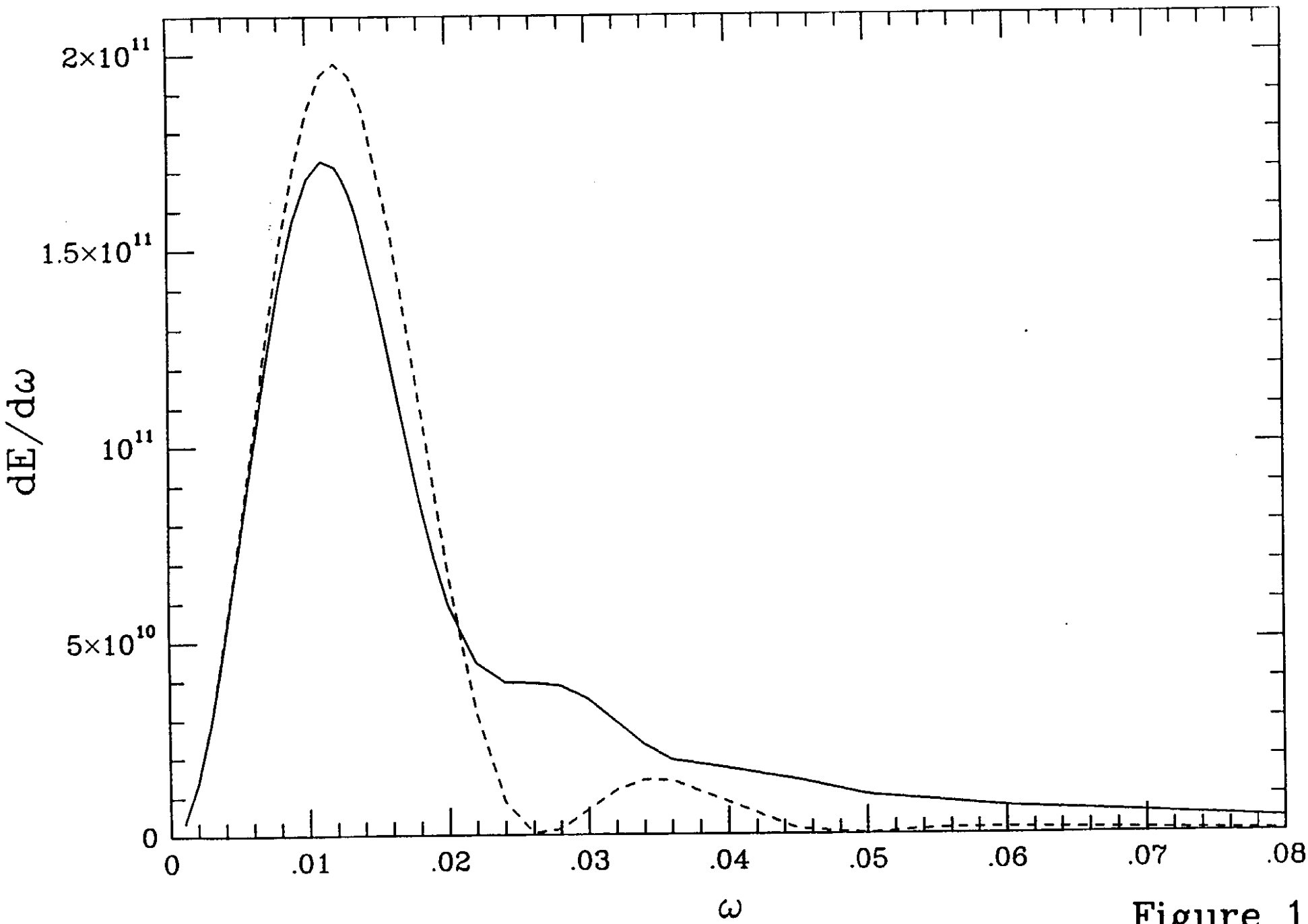

Figure 14